An updated overview of the HOLMES status

NuMass 2022 – Determination of the absolute (anti)-neutrino mass

6-10 Jun, 2022

Università degli studi di Milano-Bicocca

Matteo Borghesi

State of the art

■ To assess the mass parameter, we shall rely on non-oscillation experiments.

* Assuming ΛCDM, three neutrino species with degenerate mass ordering, a Fermi-Dirac distribution…

Cosmological measurements

- Neutrinos affect the large scale structure and dynamic of the universe by means of their gravitational interactions.
- They assume a specific theoretical model (e.g. ΛCDM cosmology)
- Parameter: $M_\nu = \sum_i m_{\nu_i}$
- Most stringent limit from Plank*: $M_\nu < 0.12$ eV

Neutrinoless double beta decay

- Extremely rare process (if exist).
- Assume neutrino as a Majorana particle.
- Parameter: $< m_{\beta\beta} > = |\sum_i U_{ei}^2 m_i|$
- Most stringent limit from KamLAND-Zen : $< m_{\beta\beta} > < 0.061 - 0.165$ eV (^{136}Xe)

*

KATRIN

- KATRIN is the ultimate spectrometer experiment.
- It started it first science run in spring 2019.
- Sensitivity goal: 0.2 eV
- The energy resolution <3 eV @18 keV.
- Background level higher than anticipated (rydberg atoms).
- First high-purity tritium campaing in 2019 results in $m_{\nu_e} < 0.8$ eV (90% CL).
- Parameter: $m_{\nu_e}^2 = m_{\bar{\nu}_e}^2 = \sum_i |U_{ei}^2| m_{\nu_i}^2$

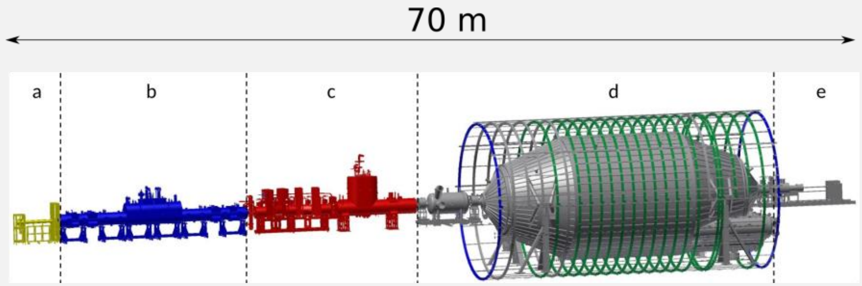

Project 8

- Ambitious experiment. New measurement technique (CRES) to measure the electron energy from tritium decay.
- Sensitivity goal: 40 meV (90% CL)
- 4 different experimental phases. Phase III ongoing…
- Energy resolution 3.3 eV @30*keV.
- Parameter: $m_{\nu_e}^2 = m_{\bar{\nu}_e}^2 = \sum_i |U_{ei}^2| m_{\nu_i}^2$

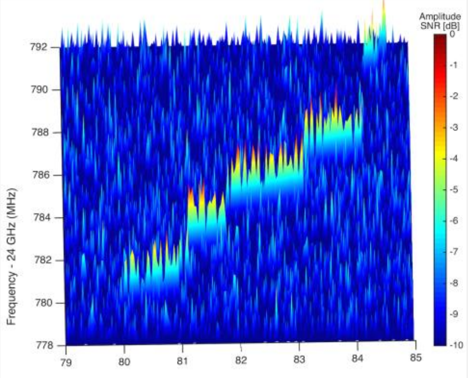

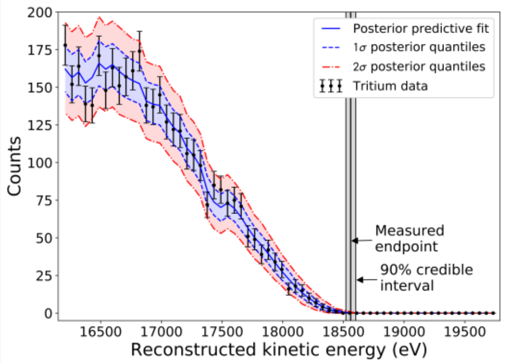

Calorimetric approach as a viable alternative to spectrometers

- **Pro:** Most of the unwanted source related effects are avoided.
- **New way to probe sub-eV neutrino mass scale?**
- A good isotope should have:
  - Low Q value
  - Proximity of a peak near the ROI
  - Short half life to reduce the experimental challenges

  → High number of events in the ROI

Ideal calorimetric experiment

- The radioactive source is embedded in the detector(s)
- Only the neutrino energy escape detection.
- Important limits on the source intensity (statistics) that can be accumulated
- Activity also limited by the relation between energy resolution and detector size.

- No convincing isotopes alternatives to $^{3}\mathrm{H}$ and $^{163}\mathrm{Ho}$ (yet).

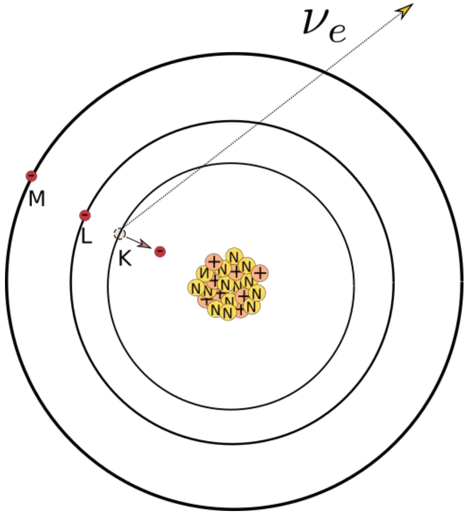

Isotope	Q value [eV]	Half life [y]	Decay	B.R	Experiments
$^{3}\mathrm{H}$	18592.01(7)	12	β^-	1	Simpson's
$^{187}\mathrm{Re}$	2470.9(13)	4.3×10^{10}	β^-	1	MANU,MIBETA
$^{163}\mathrm{Ho}$	2833(30)	4570	EC	1	ECHo, Holmes
$^{135}\mathrm{Cs}$	440	8.0×10^{11}	β^-	1.6×10^{-6}	-
$^{115}\mathrm{In}$	155	4.3×10^{20}	β^-	1.1×10^{-6}	-

EC decay of Ho & neutrino mass

- In each EC decay the emitted neutrino is recoiling against a series of states with non-zero widths.

- **At first order**, the EC of can be seen as

$$^{163}\mathrm{Ho} + e^- \rightarrow {}^{163}\mathrm{Dy}^H + \nu_e \rightarrow {}^{163}\mathrm{Dy} + E_C^H + \nu_e$$

$$\frac{d\,\lambda_{EC}}{dE_C} = \mathrm{N}(Q - E_C)\boxed{\sqrt{[(Q-E_C)^2 - m_\nu{}^2]}} \times \sum_H \frac{\varphi_H^2(0)(\Gamma_H/2\pi)}{[(E_C - E_H)^2 + \Gamma_H{}^2/4]}$$

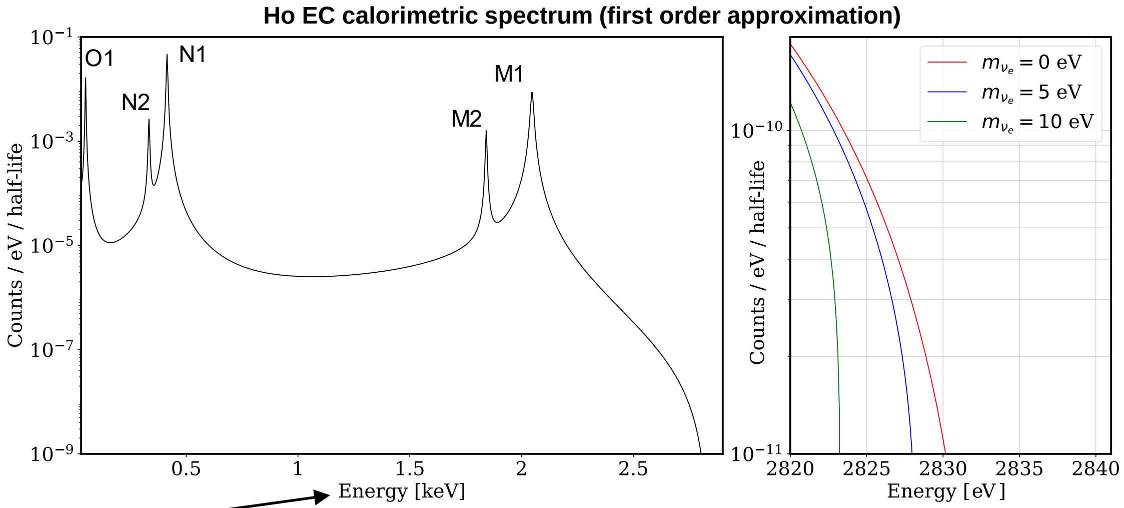

$E_c = nuclear\ recoil + \text{inner bremmstrahlung} + \text{X rays} + \text{auger electrons}$

- **However,** other contributions can not be neglected to correctly describe the spectral shape.

- *Ab initio calculation* predict several additional features.

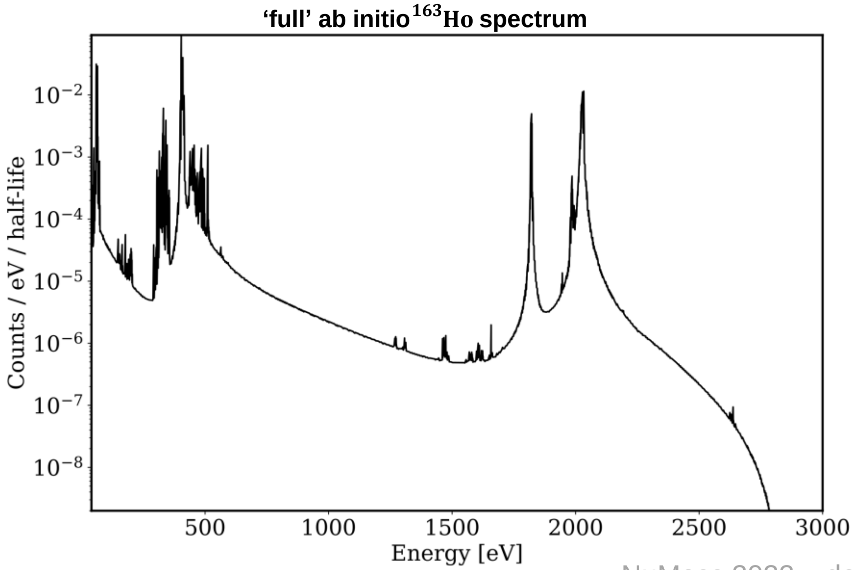

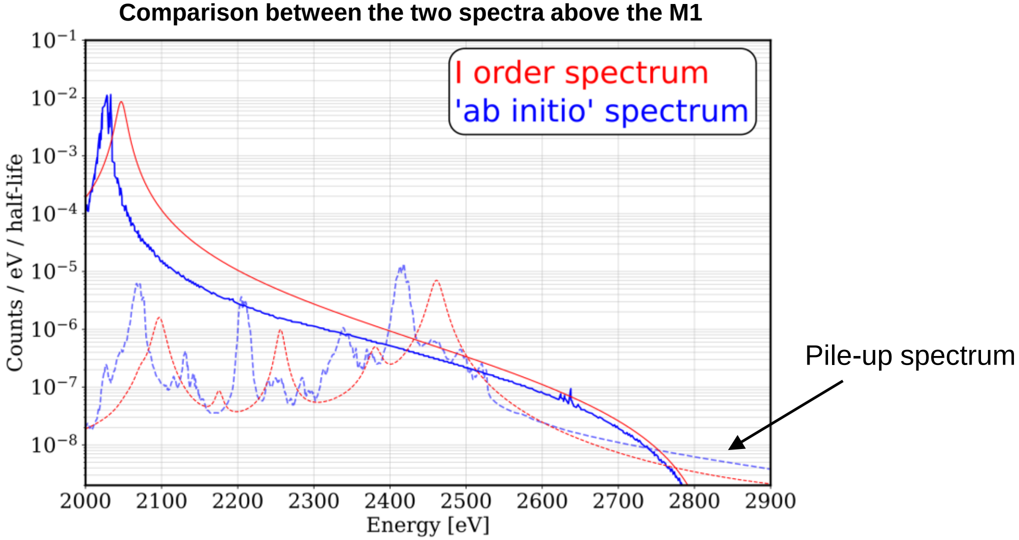

Expected sensitivity for a $^{163}\mathrm{Ho}$ calorimetric experiment

- Neutrino mass sensitivity strongly depends on the number of events at the endpoint.

$$\Sigma(m_\nu) \propto N_{ev}^{\frac{1}{4}}$$

$$N_{ev} = A\, N_{det}\, t_M$$

Single detector activity — Measurement time — Number of detectors

- A High single pixel activity (*A*) is necessary:
  - to keep the number of detector manageable
  - to reduce the complexity of the DAQ and the data analysis
  - to decrease the influence of natural radioactivity and cosmic rays

Simulation* on the neutrino mass sensitivity by varying the single pixel activity

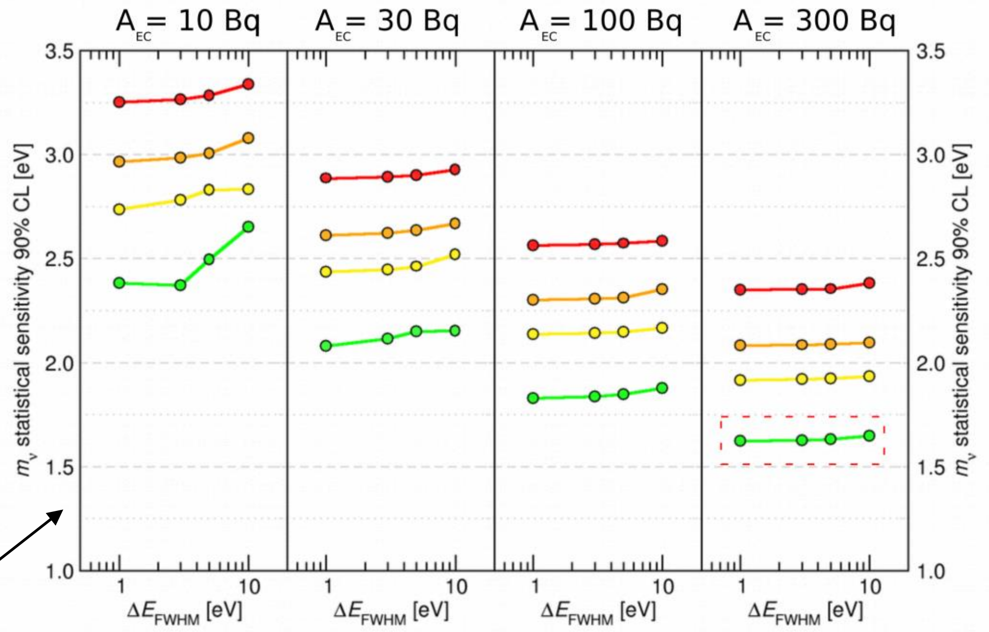

$N_{det} \times t_M = 3000\ det \times year$

Simulation* on the neutrino mass sensitivity by varying N_{ev}

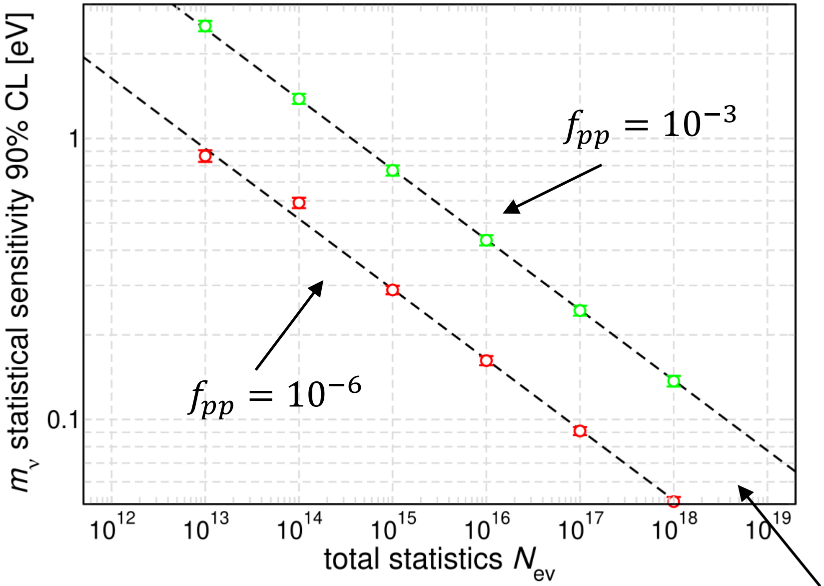

$\Delta E = 1\ eV, \tau_R = 1\ \mu s$

*Simulations performed using the first order Ho spectrum.

Holmes

- Holmes is an ambitious project that aims to verify the feasibility of the calorimetric approach to the neutrino mass determination.
- High performing detectors are needed, in terms of energy resolution ΔE and time resolution τ_R: **LTD**

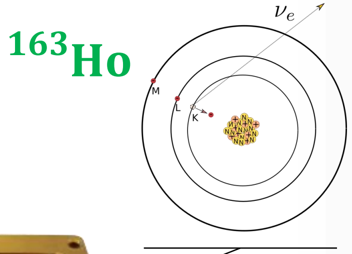

$$\left\{\begin{array}{c} \Delta E = \Delta E\ (A) \\ \tau_R = \tau_R(A) \\ \text{Custom ion implanter} \end{array}\right.$$

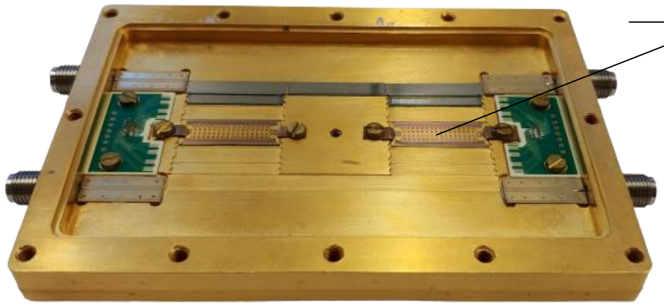

- Holmes has adopted a **high-risk/high-gain approach**.

Holmes in a nutshell

- Transition Edge Sensors (TES)
  $\Delta E \approx 1\ eV,\ \ \tau_R < 3\ \mu s$
- Microwave multiplexing readout!
- Target activity (A) of 300 Bq/det
- 6×10^5nuclei of ^{163}Ho
- 3×10^{13} events recorded in three years
- m_{ν_e} sensitivity O(1) eV

An updated overview of the HOLMES status

- Transition Edge Sensors for Holmes
  - Working principles of a TES
  - HOLMES single pixel design
  - TES array fabrication for HOLMES
- Detectors performance
- Background studies
  - Impact of natural radioactivity and cosmic rays
  - Pile-up rejection techniques

*

Transition Edge Sensor

- A TES is a superconductor film operated in the narrow temperature region between the resistive and the superconducting state ➡ The resistance is strongly dependent on temperature ➡ It is **a very sensitive thermometer**, able to detect a temperature variation of the order of a fraction of mK
- The shape of the $R_{TES}(T, I, B)$ curve depends on different things, such as: the material and the dimension of the film, the geometry of the TES, …
- The TES behavior can be described by a set of *n* differential equations:

$$\begin{cases} L\dfrac{dI}{dt} = V - IR_{sh} - IR_{TES}(T,I) \\ C\dfrac{dT}{dt} = -K(T^n - T_b^n) - K_d(T^{n_d} - T_d^{n_d}) + P_J + P \\ C\dfrac{dT_d}{dt} = K_d(T^{n_d} - T_d^{n_d}) \end{cases}$$

Thermal and electrical TES circuit

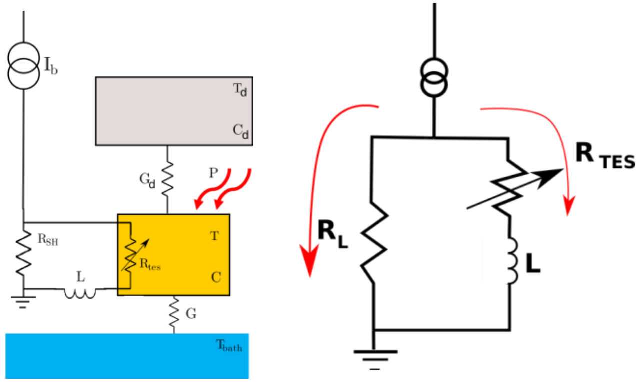

Transition shape of an Holmes-like TES

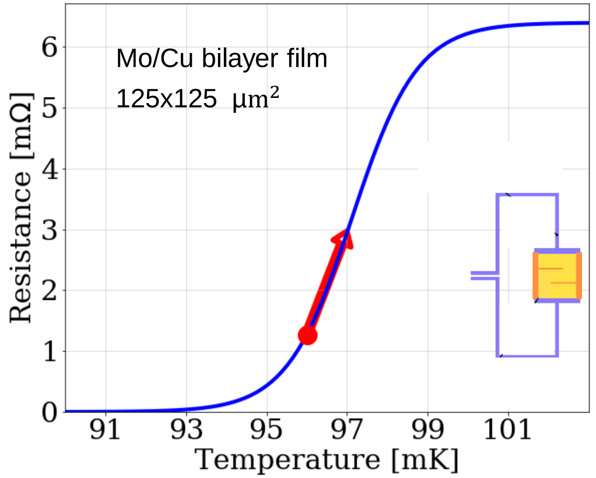

Idle current

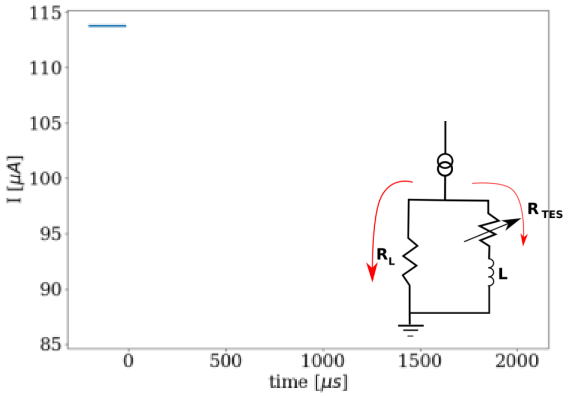

Energy release

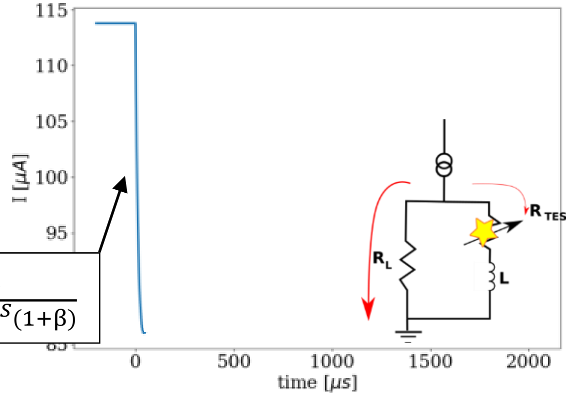

$\tau_{rise} \propto \dfrac{L}{R_L + R_0^{TES}(1+\beta)}$

Electrothermal feedback kicks in

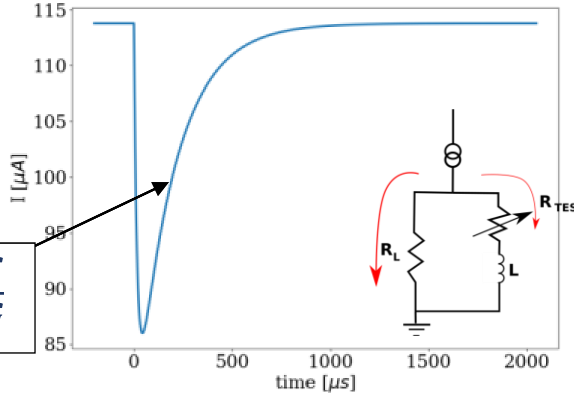

$\tau_D \propto \dfrac{C}{G}$

The TES resistance behavior is not trivial

- Two models have been developed to describe different observed TES behavior: the weak-link model and the **two fluid model**.

- When a current is flowing though the TES, a number n_{PS} equally spaced PSL will appear, resulting in a voltage drop which depends on the number of PSL.

Phase Slip Lines (PSL)

2D analogue of the of Phase Slip Center PSC): spatially localized region in which the phase of the superconducting order parameter is increasing at different rates on the two sides of the PSC.

- The model predict both the existence of bi-modal current distribution, in which the current switches between distinct current state, and the possibility of discrete variations of the TES current due to a sudden change of the PSL number.

Example of a measured IV curve (curtesy of NIST)

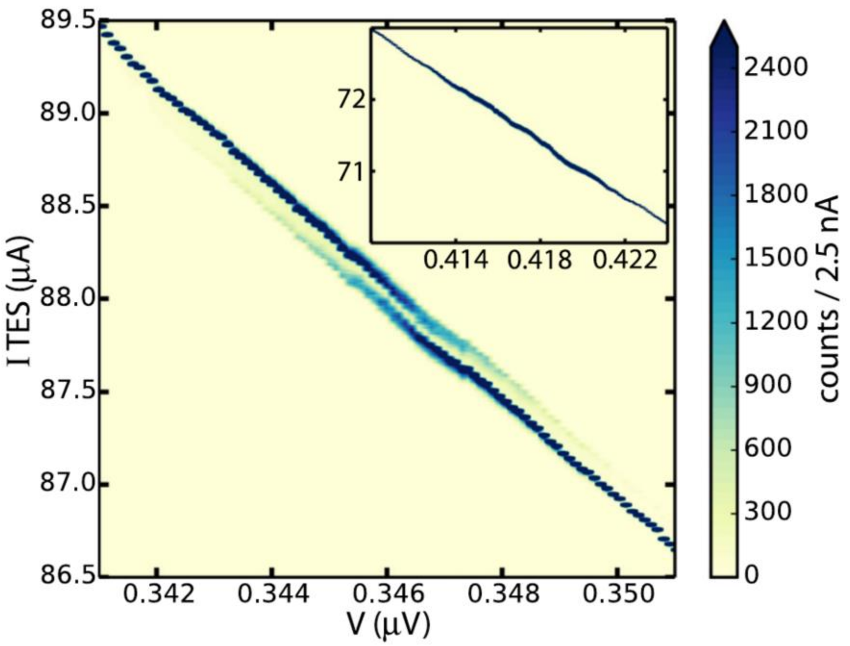

Measured step change of the detector idle current due to the variation of n_{ps}

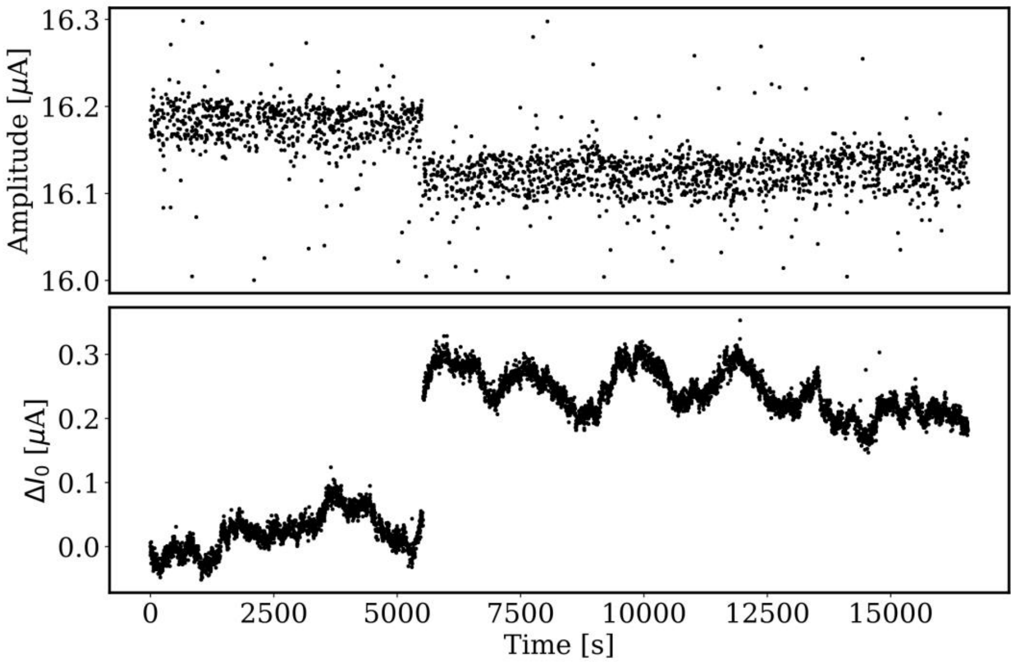

Microwave multiplexing readout

- The readout needs to satisfy both the requirements of **large bandwidth** and **high multiplexing factor**: microwave multiplexing!

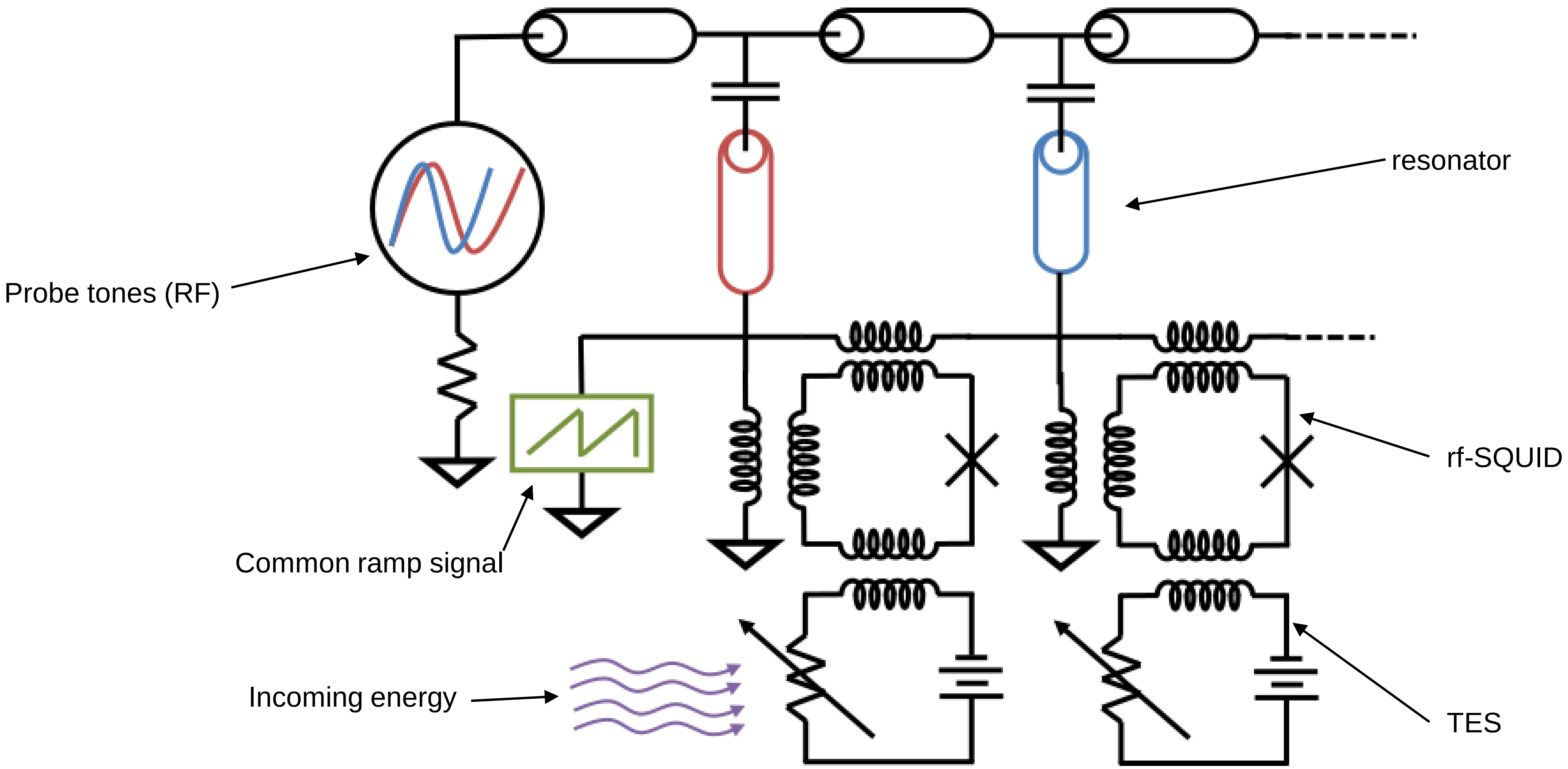

Microwave multiplexing readout

■ The readout needs to satisfy both the requirements of **large bandwidth** and **high multiplexing factor**: microwave multiplexing!

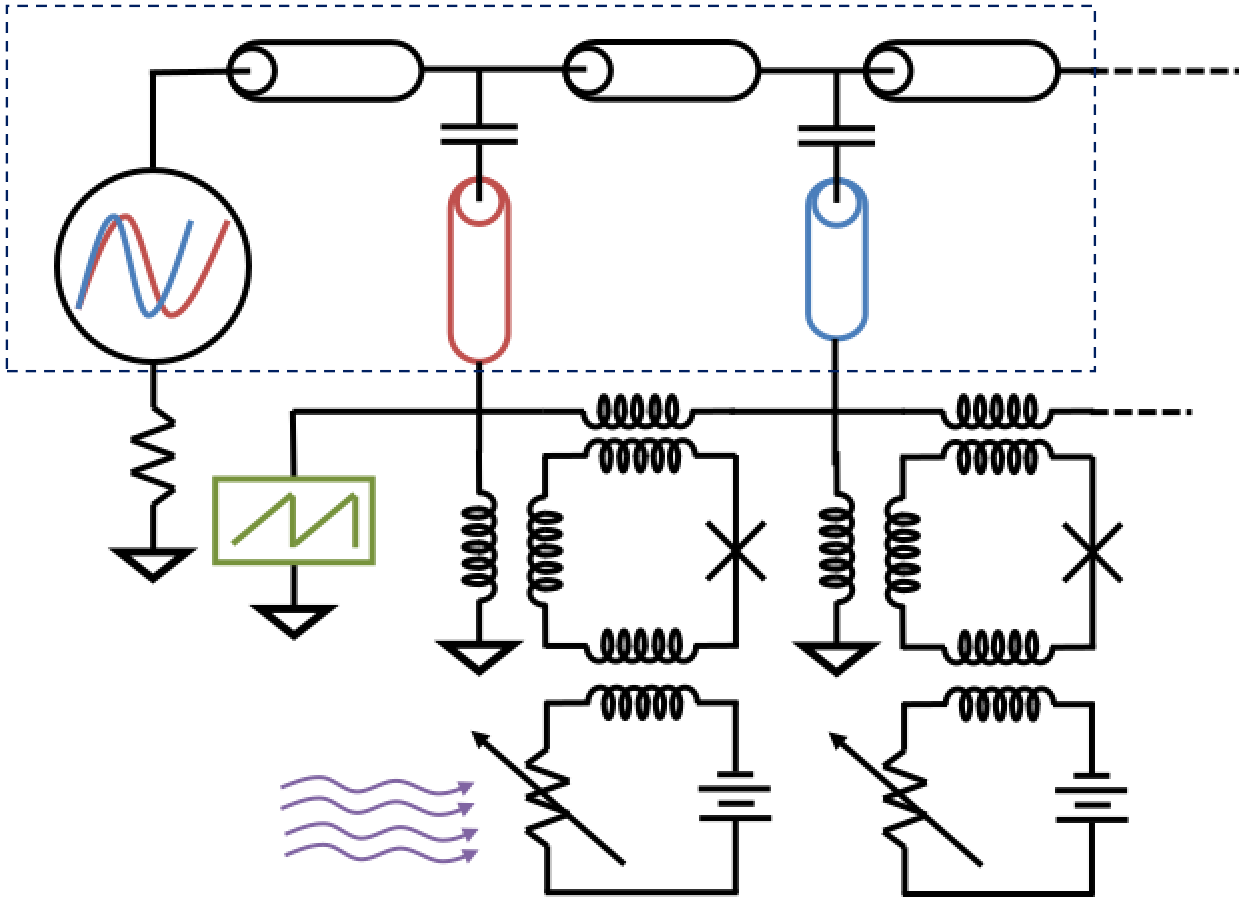

RF line: resonators and probe tones

- Quarter wave resonator capacitatively coupled to a feed-line.
- All the frequency different from f_{res} will be transmitted unaffected.

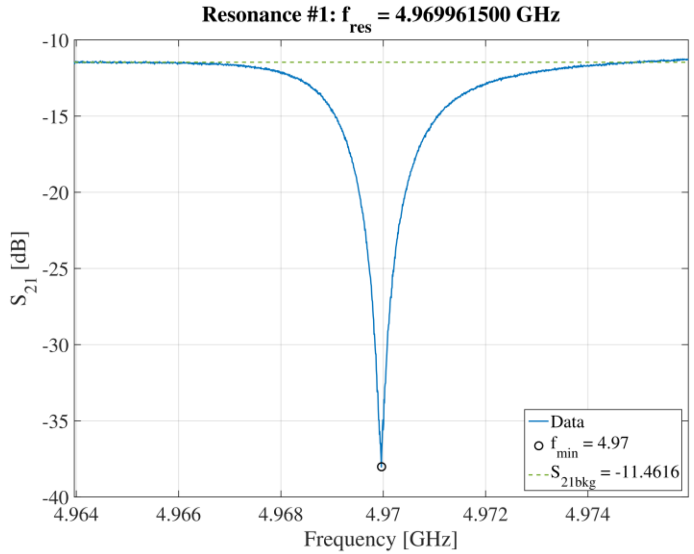

Microwave multiplexing readout

- The readout needs to satisfy both the requirements of **large bandwidth** and **high multiplexing factor**: microwave multiplexing!

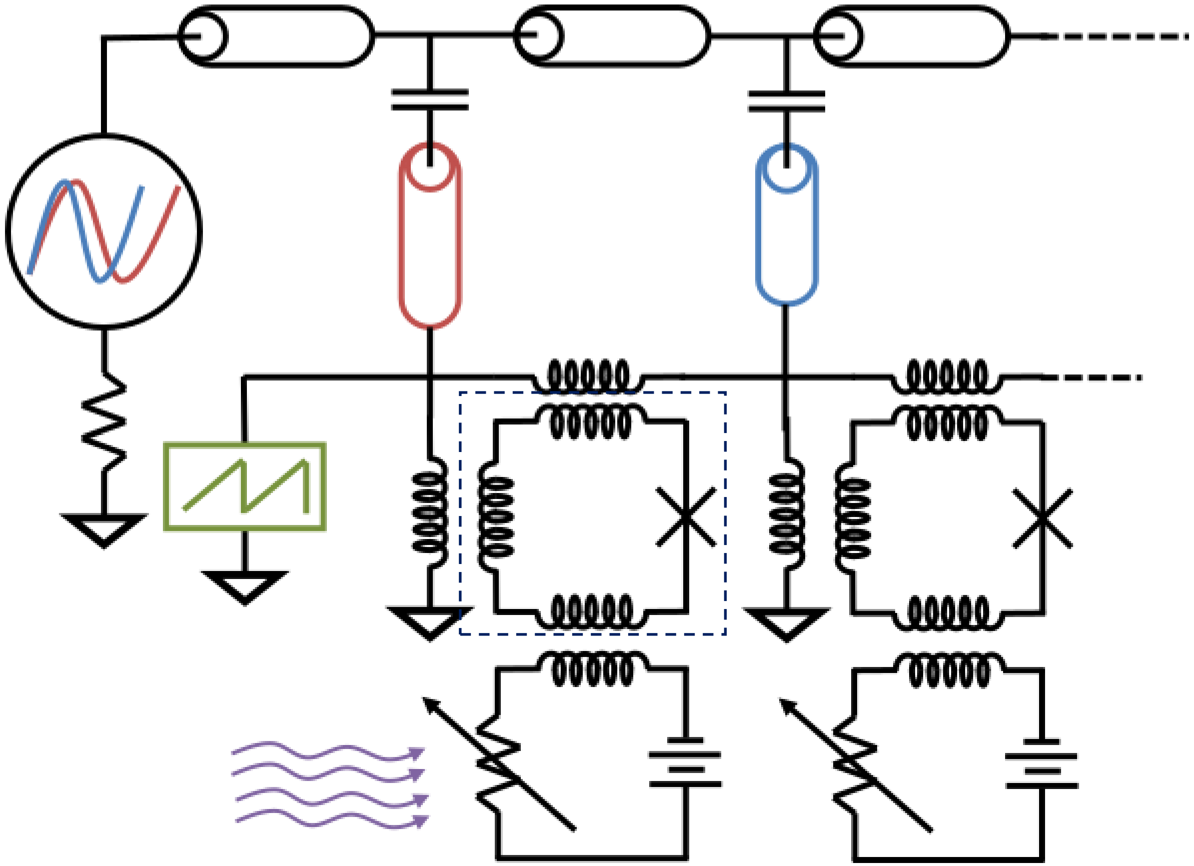

Rf-SQUID

- rf-SQUID are sensitive magnetometers which measure the magnetic flux.

Picture of the Holmes rf-SQUID

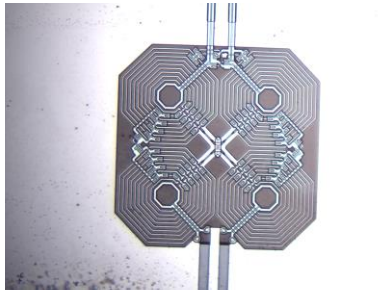

- Their response to the variation of the magnetic flux is a non invertible function.

Measured variation of the resonant frequency of one of our resonator

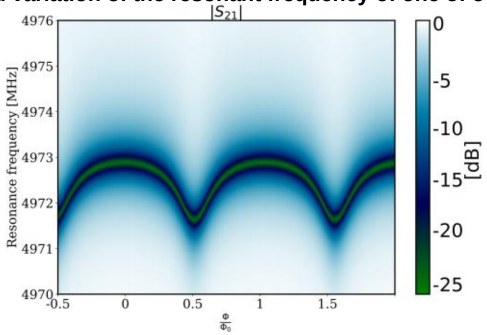

- When coupled to a resonator, the resonance frequency will shift with the magnetic flux.

Microwave multiplexing readout

- The readout needs to satisfy both the requirements of **large bandwidth** and **high multiplexing factor**: microwave multiplexing!

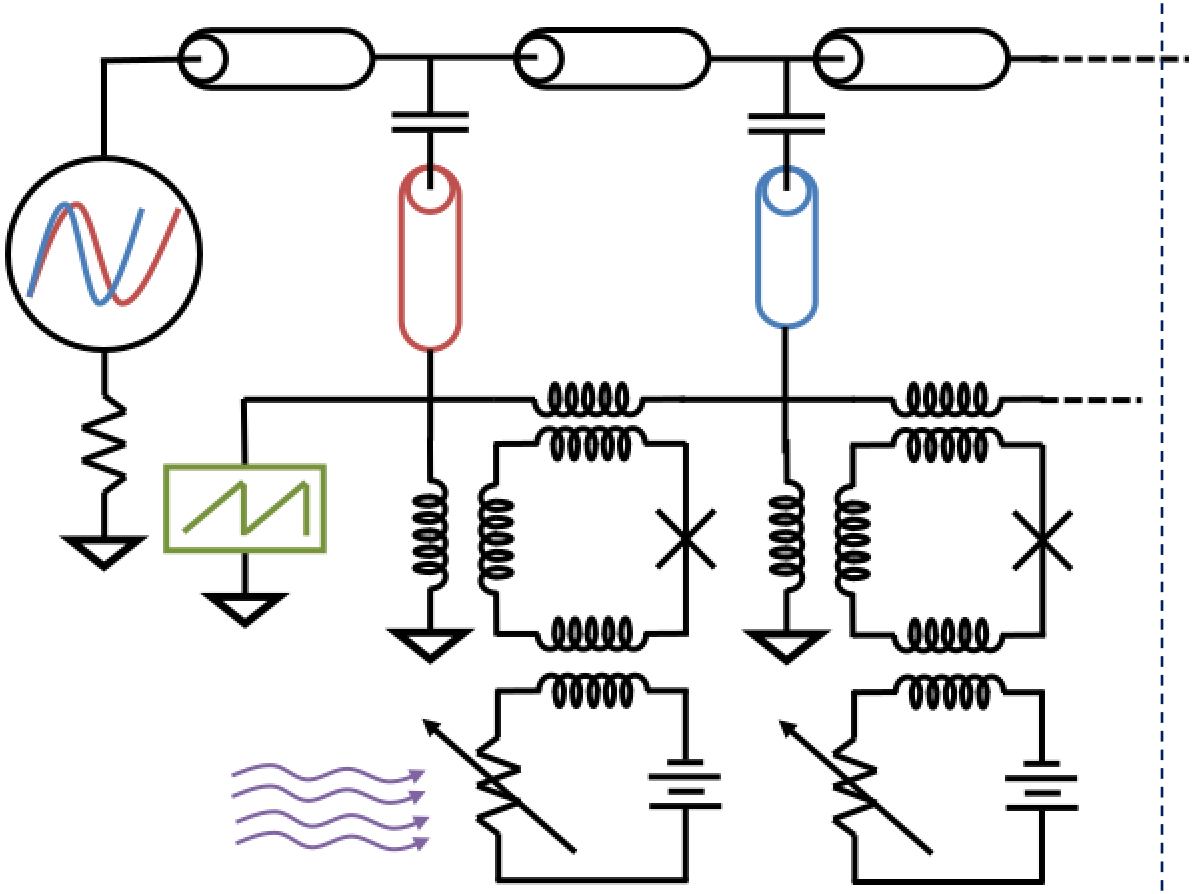

Putting all together

- The flux ramp is a sawtooth signal that force the rf-squid to oscillate a certain number of times.
- Under certain condition, a variation of the TES current will look like an offset of the phase in the periodic ramp-induced SQUID oscillations.
- TES signal → dephasing event

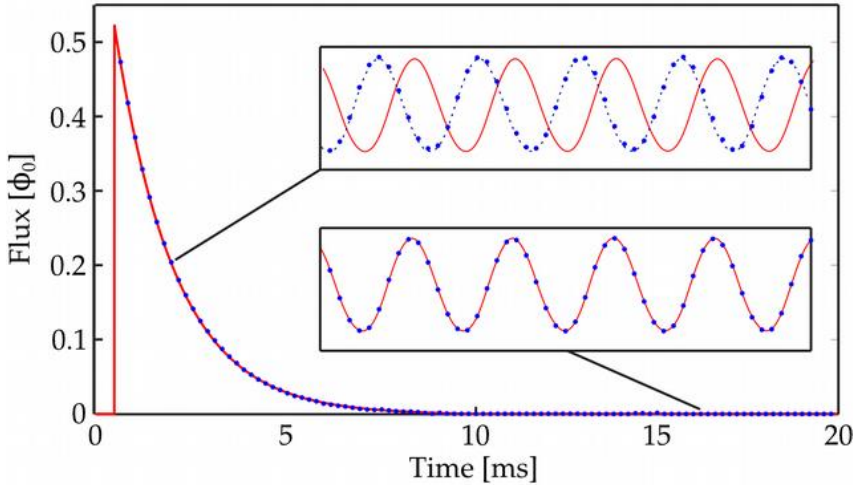

$$E \rightarrow \delta T_{TES} \rightarrow \delta I_{TES} \rightarrow \delta \Phi_{squid} \rightarrow \delta f_{resonator}$$

Holmes detector design

- Proper detector design found after an intensive measurement campaign.

  Alpert, B., et al. "High-resolution high-speed microwave-multiplexed low temperature microcalorimeters for the HOLMES experiment." EPJC

- TES + absorber with a sidecar geometry.

- Au absorber $200 \times 200 \times 2\ \mu m^3$. The probability that the electrons (photons) from the $^{163}\mathrm{Ho}$ decay are stopped is predicted to be 99.99% (96.73%).

- The TES surface is shaped using copper bars (increase ETF and reduce the excess electrical noise).

- SiN membrane + copper perimeter to control the thermal conductance toward the thermal bath *G*.

  Phonon propagation in the membrane close to the 2D regime.

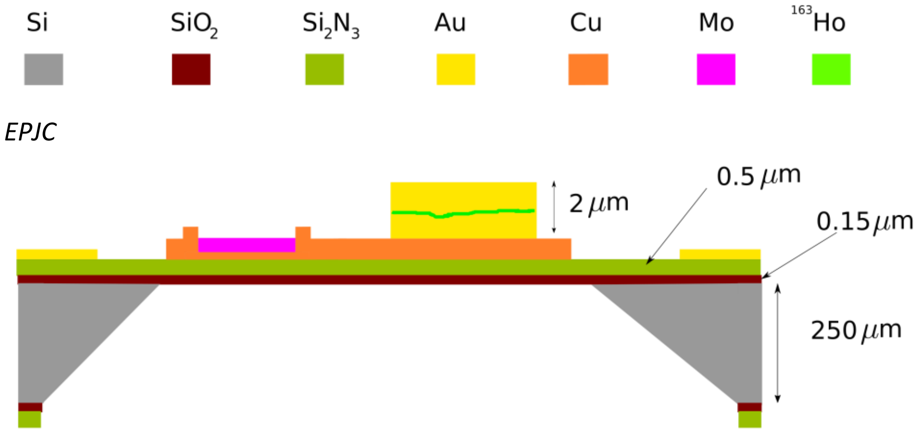

Sideview and topview of the Holmes detector design

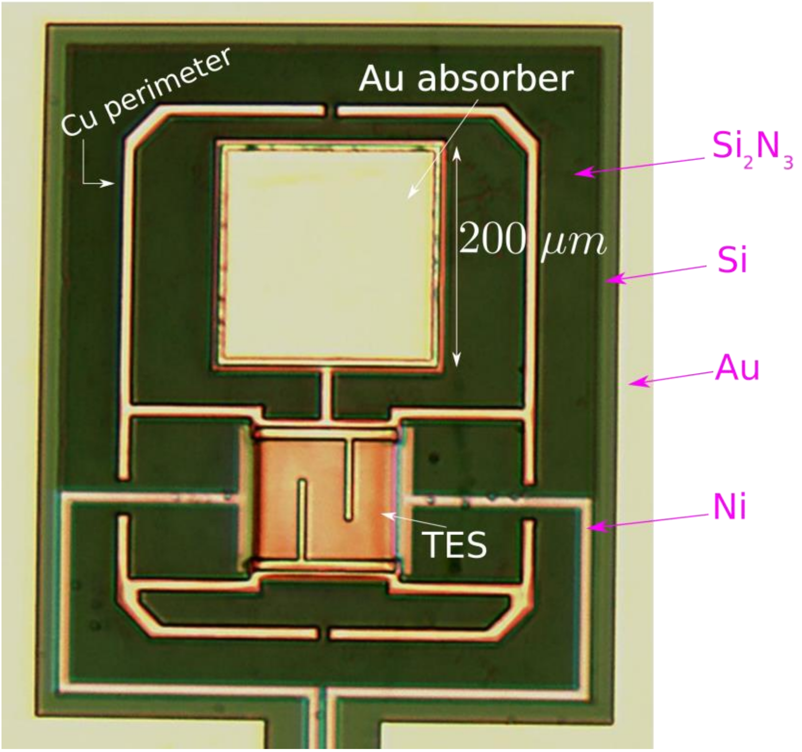

Holmium production and purification

- Holmes needs ~ 300 MBq of $^{163}\mathrm{Ho}$ for 1000 detectors

- $^{163}\mathrm{Ho}$ has to be produced via neutron irradiation (@ILL, Grenoble (Fr), thermal neutron flux $\sim 1.3 \times 10^{15} \mathrm{n/s/cm^2}$)

$$^{162}\mathrm{Er_2O_3} \quad \Rightarrow \quad ^{162}\mathrm{Er(n,\gamma)}\ ^{163}\mathrm{Er} \rightarrow {}^{163}\mathrm{Ho} + \nu_e$$

- Chemical purification @PSI before and after the irradiation

200 MBq available and now stored @Genova

Holmes array fabrication

- The Holmes detectors have to undergo different fabrication steps in order to have the ^{163}Ho implanted inside the gold absorbers.

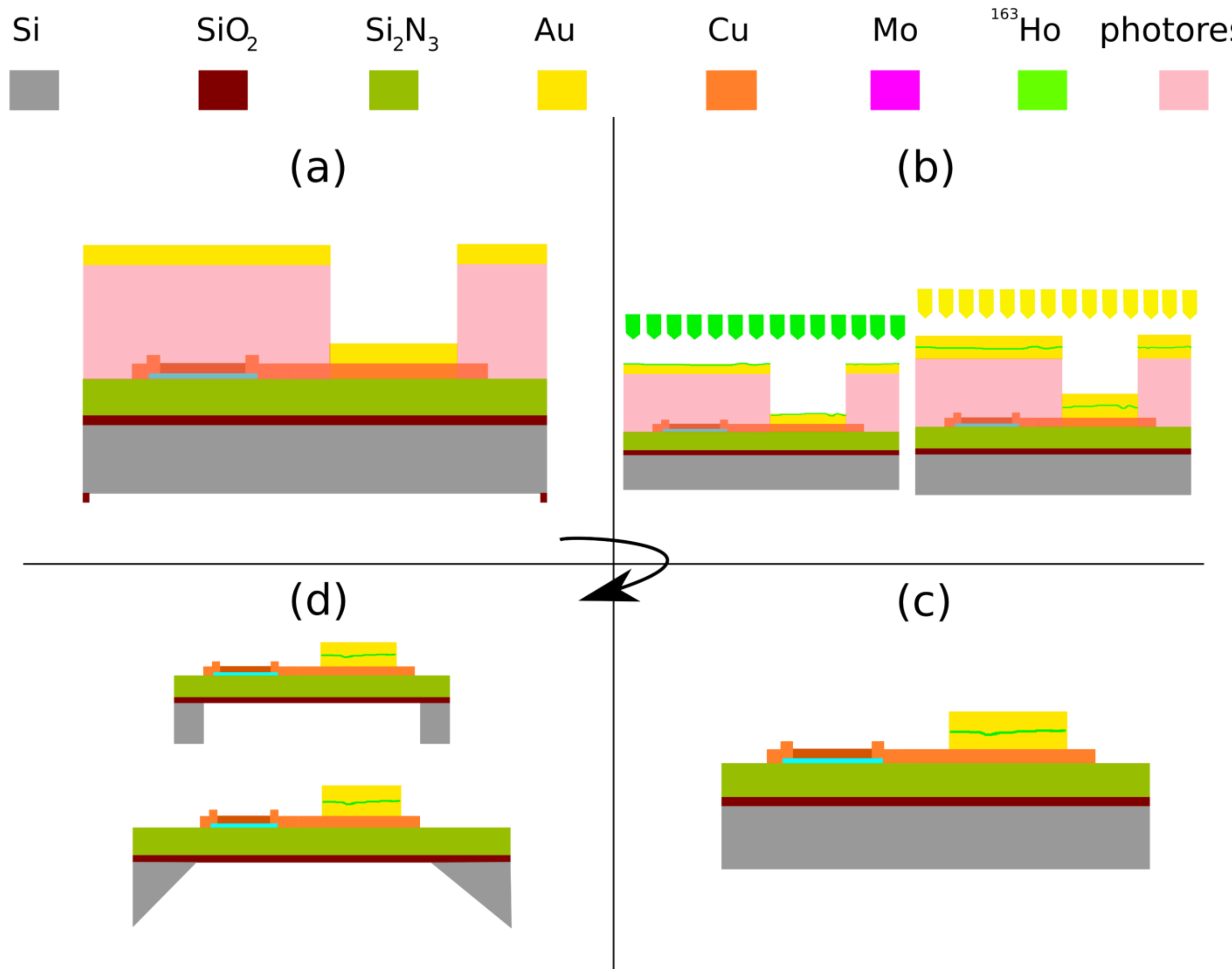

Holmium implantation

- Designed to embed the holmium inside the detectors' absorbers and to perform a mass separation of the $^{163}\mathrm{Ho}$ from the other contaminants.

- **Sputter ion source** is the most critical component of the implanter.

Ion implanter

- Extraction voltage 30-50 kV (10-100 Å implant depth)
- Main components: argon penning sputter ion source, magnetic dipole mass analyzer ($B_{max} = 1$ T), faraday cup and slit.
- $^{163}\mathrm{Ho}/\,^{166m}\mathrm{Ho}$ separation better than 10^5
- Optical fiber control

Faraday cup behind the slit to calibrate the dipole magnet.

Schematic of the ion implanter

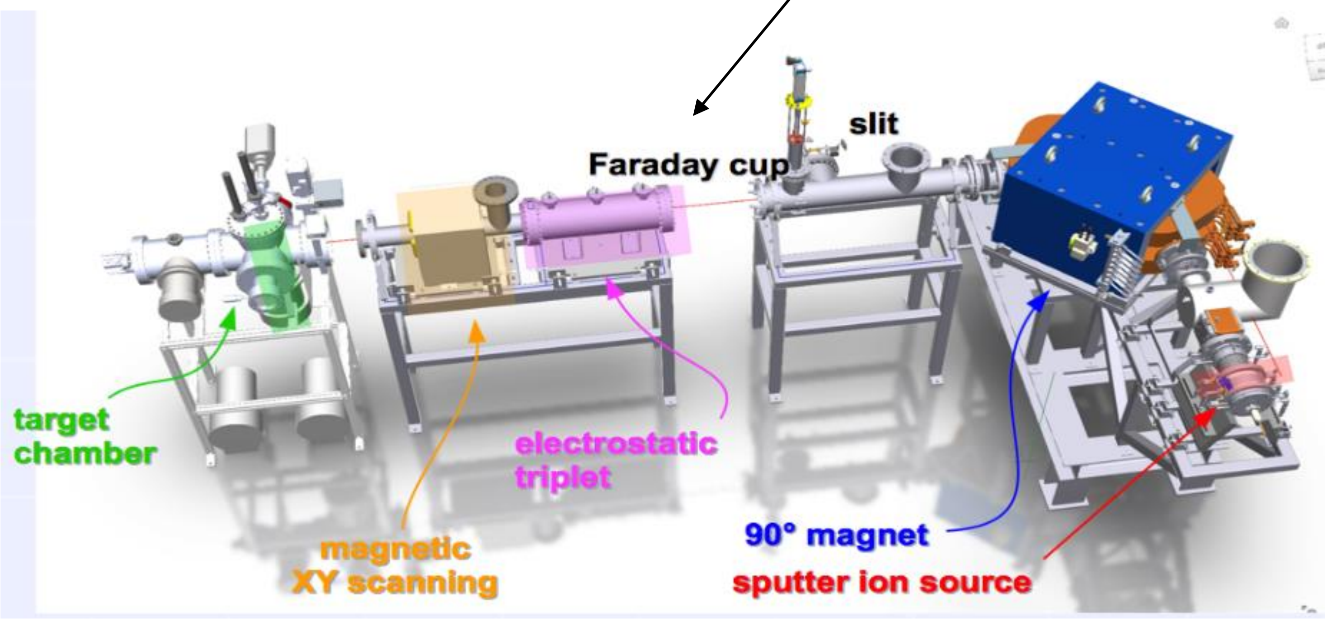

Cu spectrum

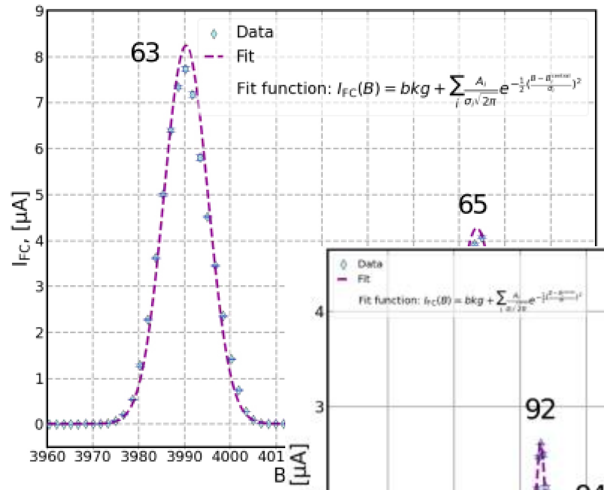

Mo spectrum

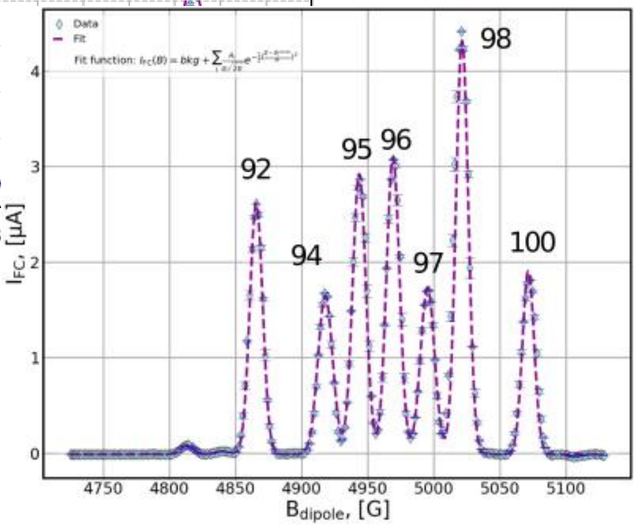

Holmium implantation

- Many efforts were put to install the refrigeration system with de-ionized water, setup the grounding of all the HV components and to optimize the beam parameters.
- Currently the experimental efforts are put to build the most suitable target for the Ho sputtering.
- We are testing three techniques for sputter target fabrication:

Schematic of the sputter ion source

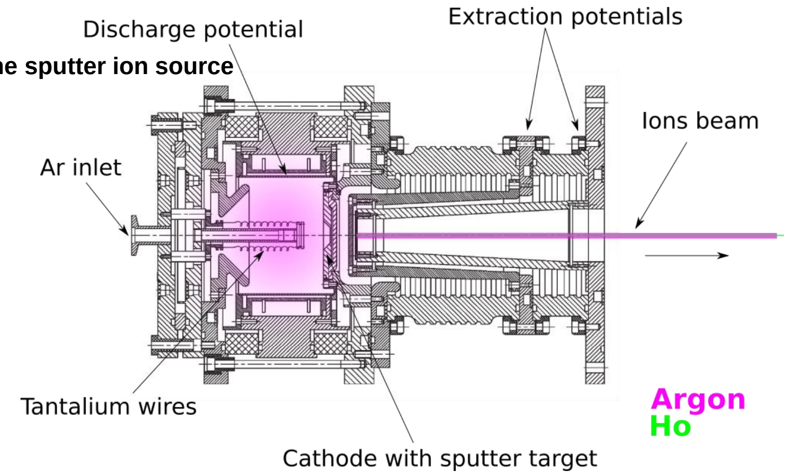

Molecular plating

High yield (>90%) electrodeposition from organic solvent

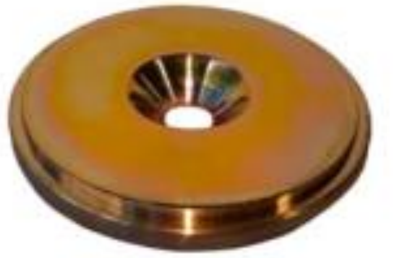

See Mariia Fedkevych's talk 163Ho implantation in the Holmes experiment

Coupled reduction on molecular plating

Ho reduction and diffusion into a substrate (Pd). Formation of intermetallic compound.

Sintered target

$Ho(NO_3)_3$ in a metallic mixture of Zr and Y fine-grained powder.

Best current-stability: *O*(200) nA over 15 h!

Au deposition test: commissioning

- Test goals:
  1. Beam parameters optimization
  2. Calibration
  3. Deposition rate estimation
  4. Evaluation of the uniformity of the sputtered gold

Why Au co-evaporation?

- $^{163}\mathrm{Ho}$ concentration in absorber saturates
- Au deposited in situ to avoid oxidation
- Heat capacity

- 4 COMIC microwave sources
  - **4 argon beams**
  - **4 Au targets**
  - Increase deposition uniformity
  - Increase deposition rate

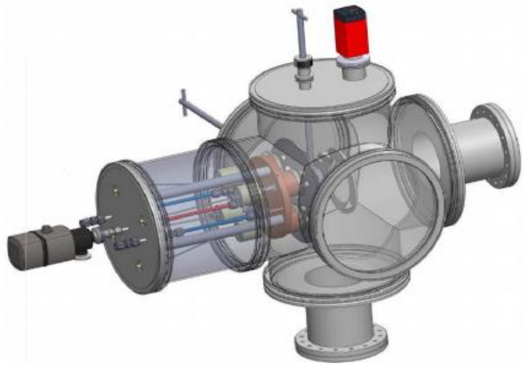

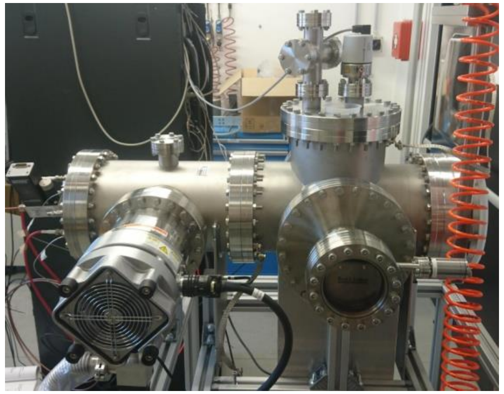

- Target chamber pressure $\sim 10^{-8}$mbar
  Total Ar ion current achieved $\sim 250\ \mu A$
  Rate measured with a quartz microbalance near the target

- With a $\sim 250\ \mu A$ total Ar current

$$< \text{rate @ microbalance} > = 39 \pm 2\ nm/h$$
$$< \text{rate @ target} > = 52 \pm 4\ nm/h$$

$\sim 20\ h$ for 1 μm Au deposition

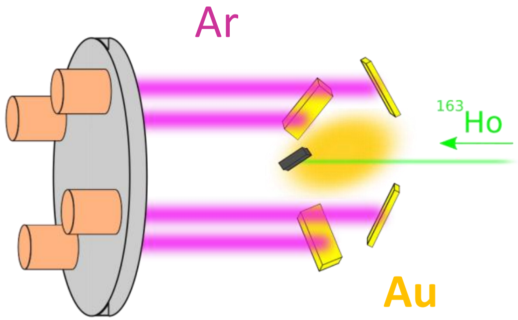

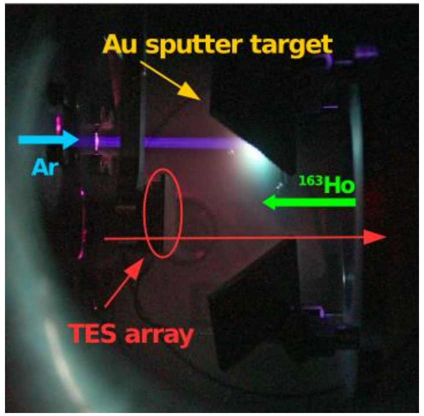

Au deposition test: uniformity and lift-off

- Au sputtered for 22 hours on a Si slab $1 \times 1\ cm^2$
  With a shadow mask with 9×9 holes on top
- The thickness in the center of the circles were measured with a profilometer.

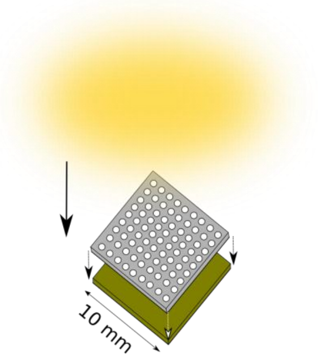

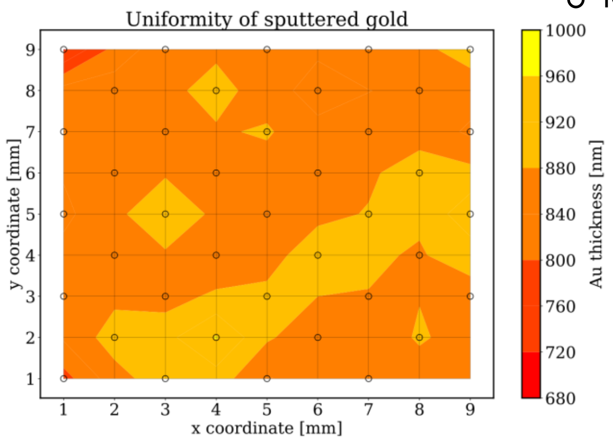

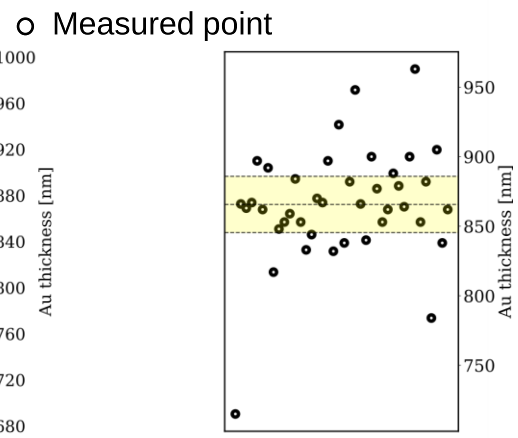

The deposited gold should be **uniform** all over the TES array.

- After the gold deposition of the absorbers, the photoresist mask (7 μm thickness) must be removed.

Sample in acetone (40 °C) for 24h

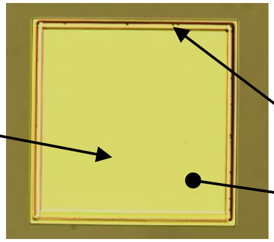

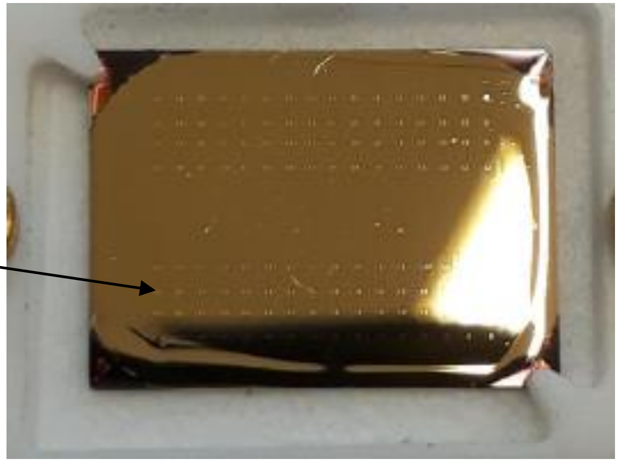

After the lift-off, the Au deposited **remains only** on the absorbers.

Membrane release

Silicon Deep Reactive Ion Etching (DRIE)

- Best for close packing and high implant efficiency
- Not properly tuned (yet)

Calculated ^{163}Ho beam FWHM

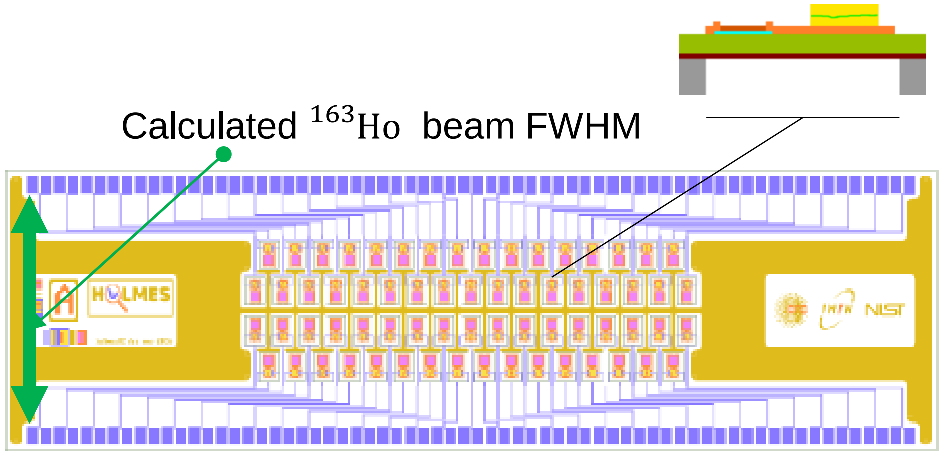

Back of the detector chip after DRIE etching

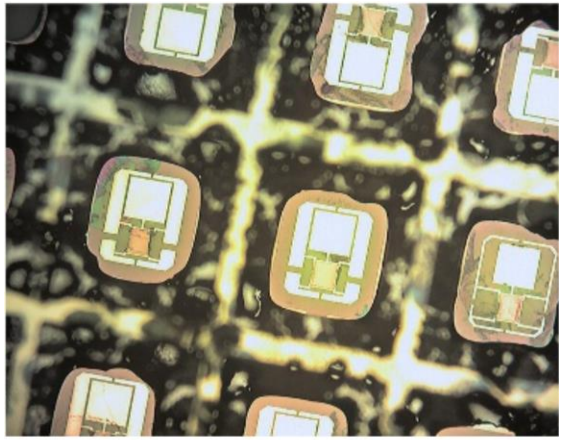

Silicon KOH anisotropic wet etching

- Requires more spacing between the pixels
- **Succesfully tested**

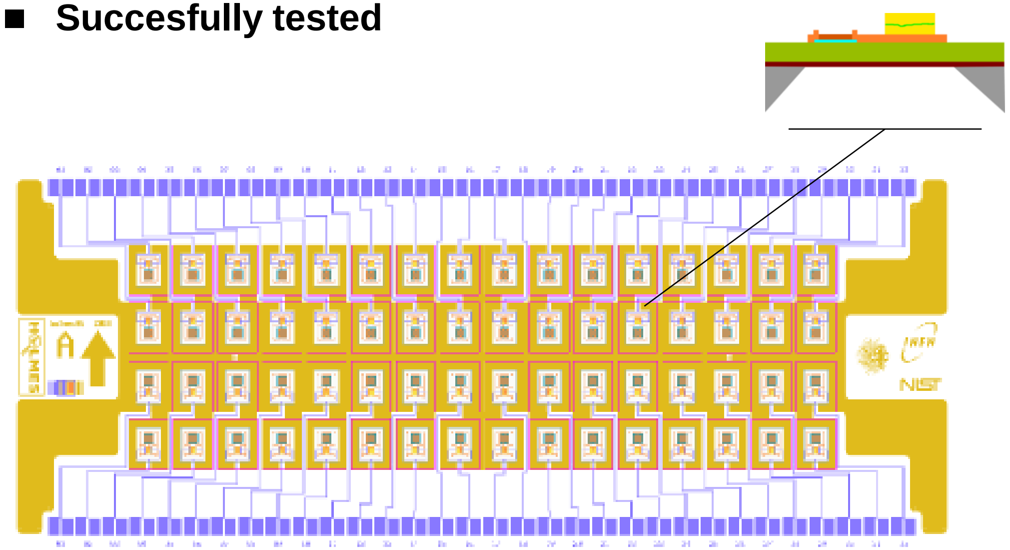

Back of the detector chip after KOH etching

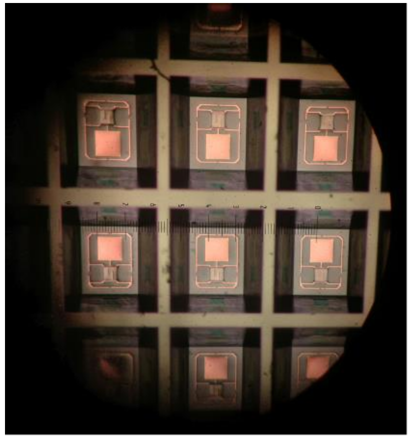

Membrane release: KOH

- Potassium hydroxide (KOH) displays an etch rate selectivity dozens of times higher in <100> crystal directions than in <111> directions

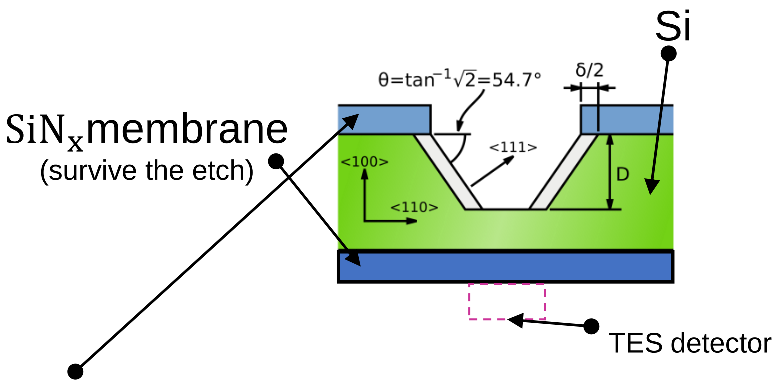

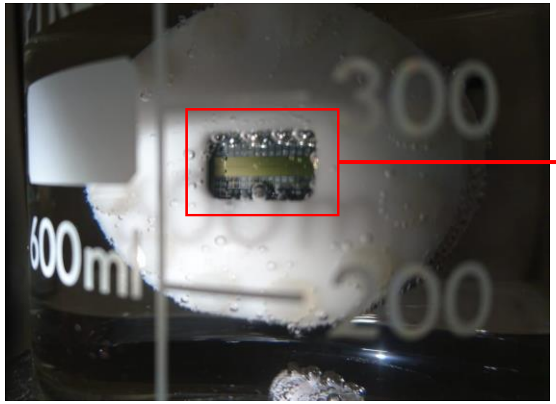

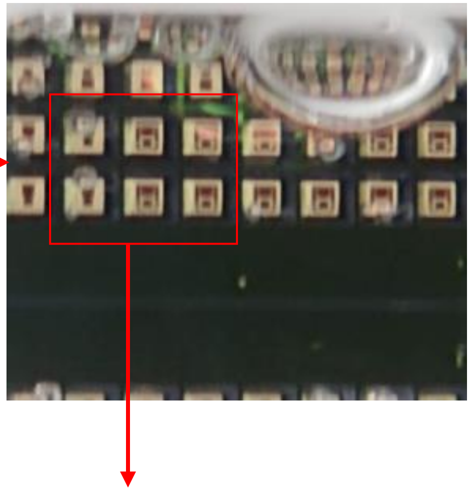

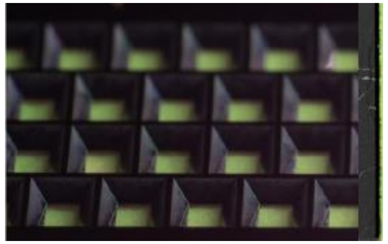

New SiNx mask was designed at NIST to match the thermal performance of the DRIE array

- The TES arrays were placed in a 33% KOH with isopropanol solution
  - smoothen the <100> surface
  - increase the anisotropy in the etch

↓

Estimated ETCH rate @ 80 ̊C~ 1 μm/minute

- The temperature was mainteined 65 ̊C <T< 70 ̊C to avoid turbolent motion in the solution

↓

Silicon etch rate $\cong 40-45\ \mu m/h$

From raw data to ‘clean’ calibrated spectrum

First level data reduction

↕

Evaluation of pulse information

↓

Energy estimation

- Optimum filter
- Arrival time correction
- Gain drift correction
- Energy calibration

↓

Second level data reduction

- The analysis of microcalorimeters designed for X-rays requires grate care, because their excellent intrinsic energy resolution can hardly be achieved without an accurate analysis.
- The data from each pixel need to be processed separately.

See Luca Origo’s talk
Data analysis tools for the Holmes experiment

The Watson software

- Software for LTD data analysis
- Object oriented programming. Written in python (numpy and scipy), but still very fast!
- Easy to read, easy to fix code
- GUI with QT5 for handy day to day operations
- Data are stored in hdf5 (hierarchical, filesystem-like data format)

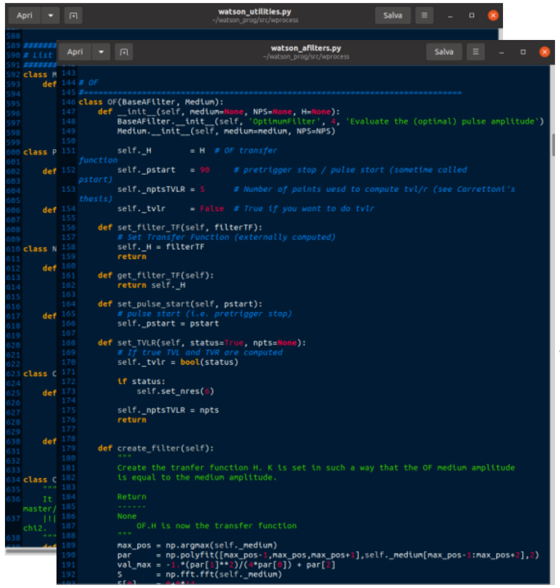

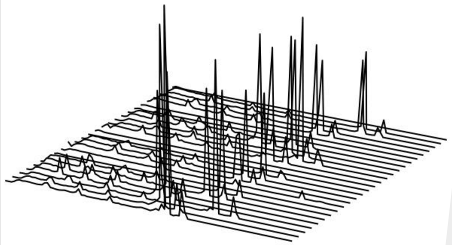

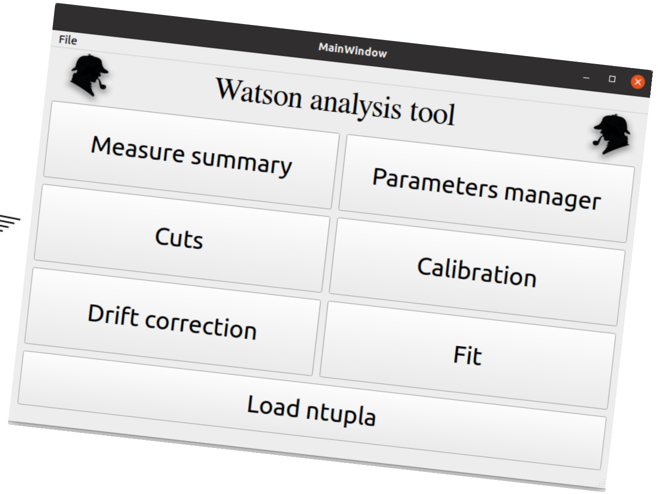

Overview of the measurement @Bicocca

- Different array configurations where tested:
  - *holmesDRIE*: baseline array developed at NIST ($2\ \mu m$ thick absorbers @NIST ⊕ DRIE Si etching @ NIST)
  - *holmesKOH*: prototype array ($2\ \mu m$ thick absorbers @NIST ⊕ KOH Si etching @ Unimib)
  - *holmesKOHAu: final array configuration* ($2\ \mu m$ thick absorbers @ Unimib ⊕ KOH Si etching @ Unimib)

- **Array performance tested without $^{163}\mathbf{Ho}$**

- External X rays source: two $^{55}\mathrm{Fe}$ sources pointing at a mixture of NaCl and $\mathrm{CaCO_3}$
  - X rays in the energy range of interest of Holmes

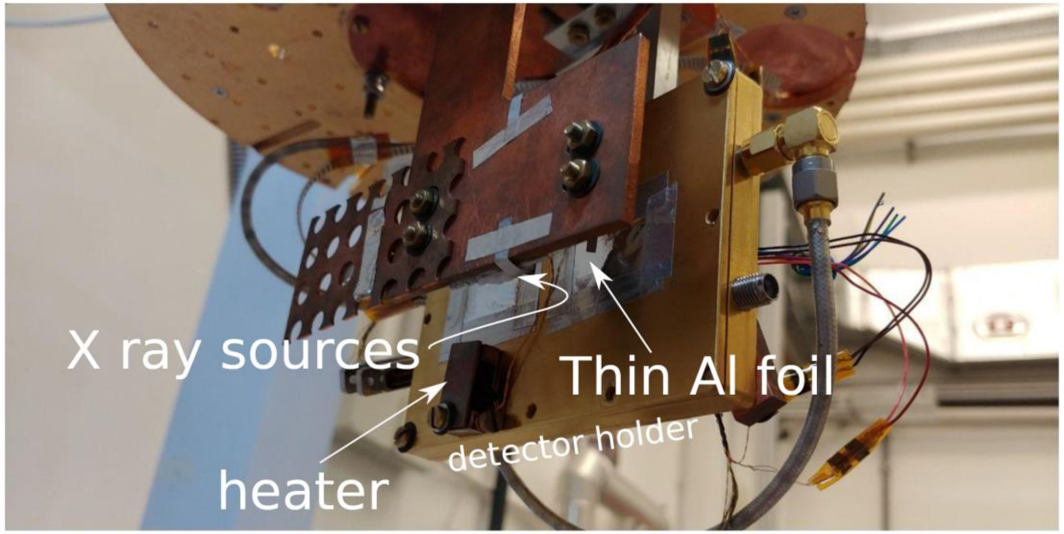

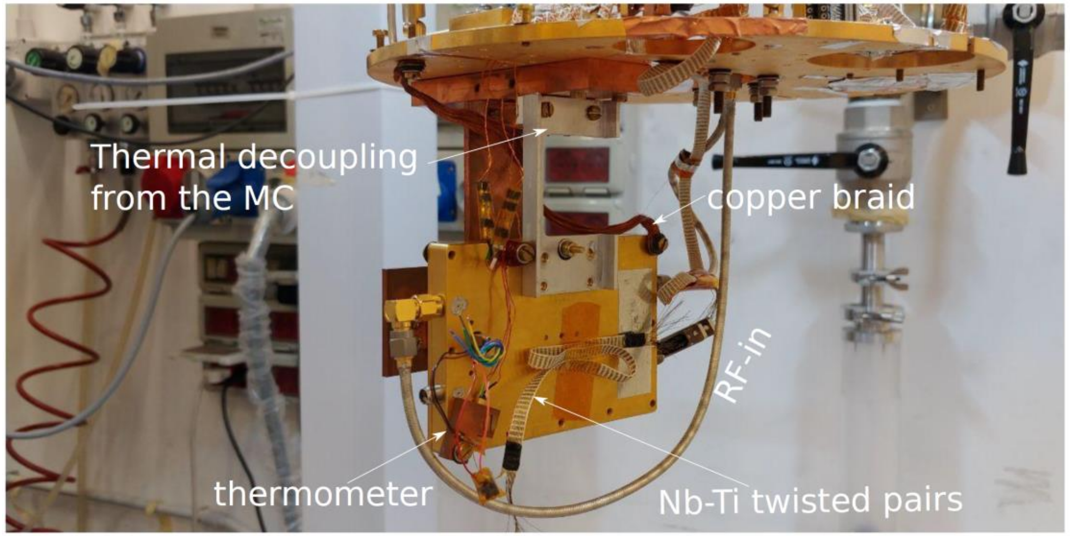

Cryogenic and warm electronics setup

- $^{3}\mathrm{He}/\,^{4}\mathrm{He}$ diluition refrigerator (200 μW of cooling power @100 mK)

- Low noise HEMT amplifier @2K
  constant gain in the BW of the Holmes resonators, 4-8 GHz)

- Multiplexing is based on a heterodyne mixing scheme, with a ROACH2 readout system

Holmes setup

- **Now**: 1 detectors box (128 pixels max, 2 rf-cables, 1 HEMT)
- **Final**: 8 detectors box (1024 pixels, 8 rf cables, 4 HEMT)

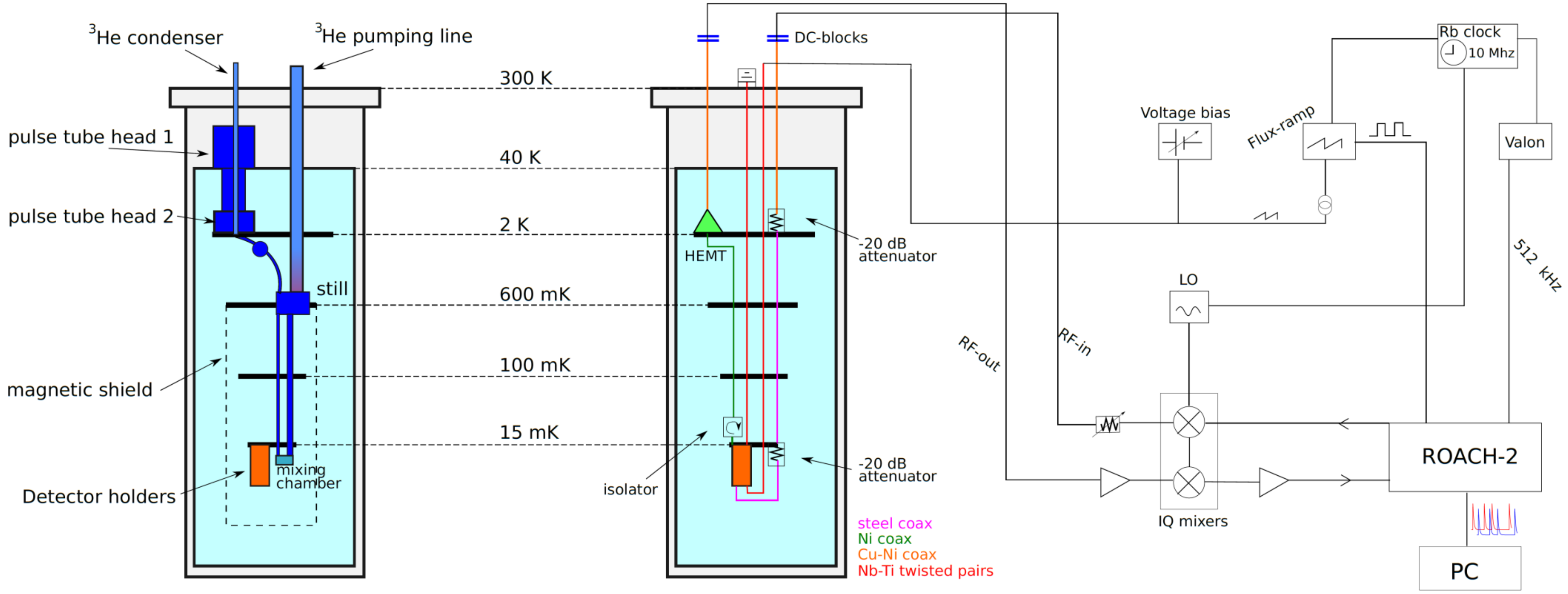

Holder setup

- Each holder is hosting 2 detectors array (4×32 pixels), for a total of 128 detectors with their readout and bias chips.

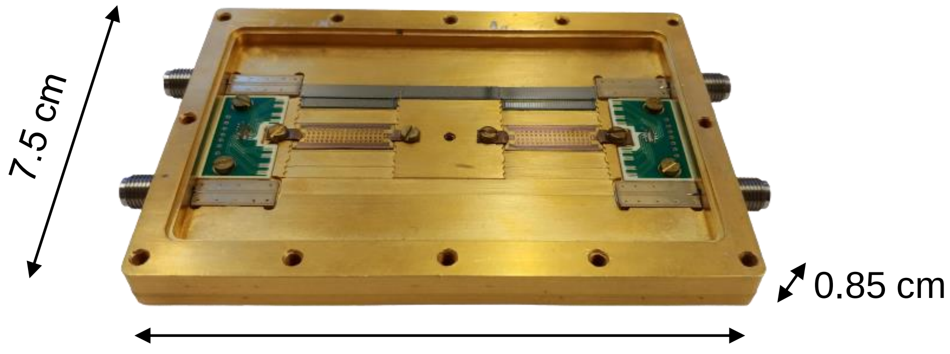

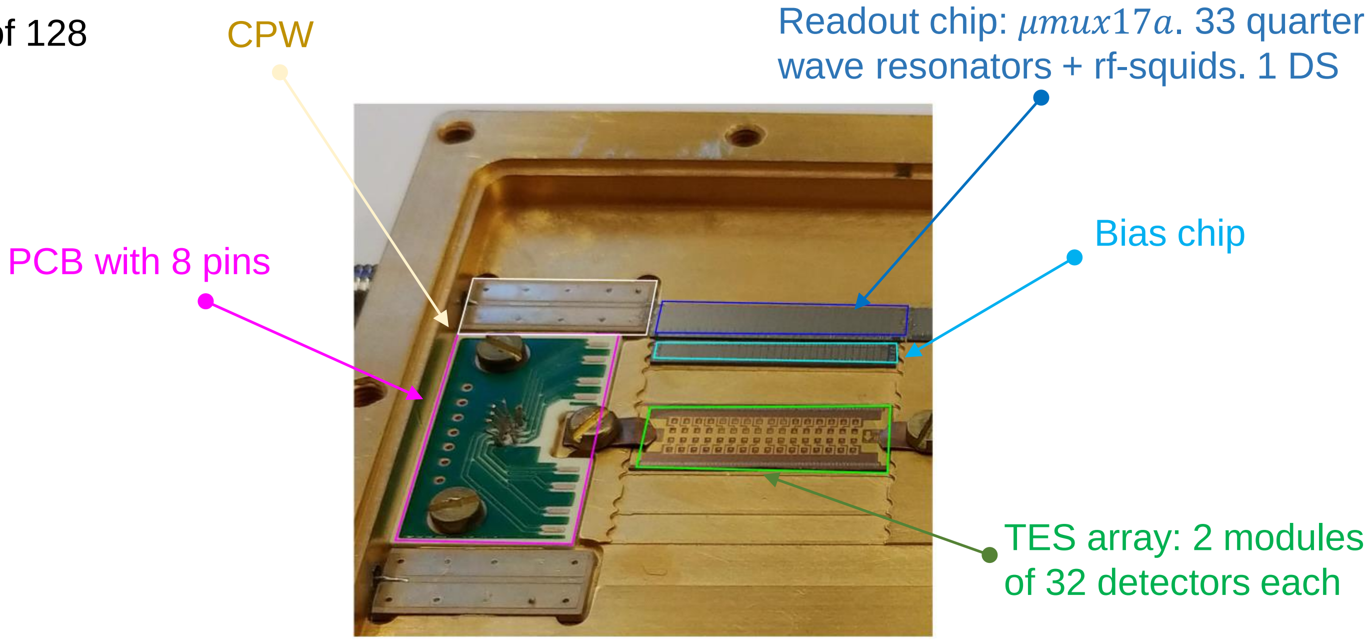

- Measured ‘’only’’ 32 detectors each time.

Holmes readout is based on modules of 32 channels each. If one is able to correctly readout one single module, increasing the number of detectors is just a matter of increasing the number of modules.

Example of the resonances profile before and after the air-bridges bonding across the feedline

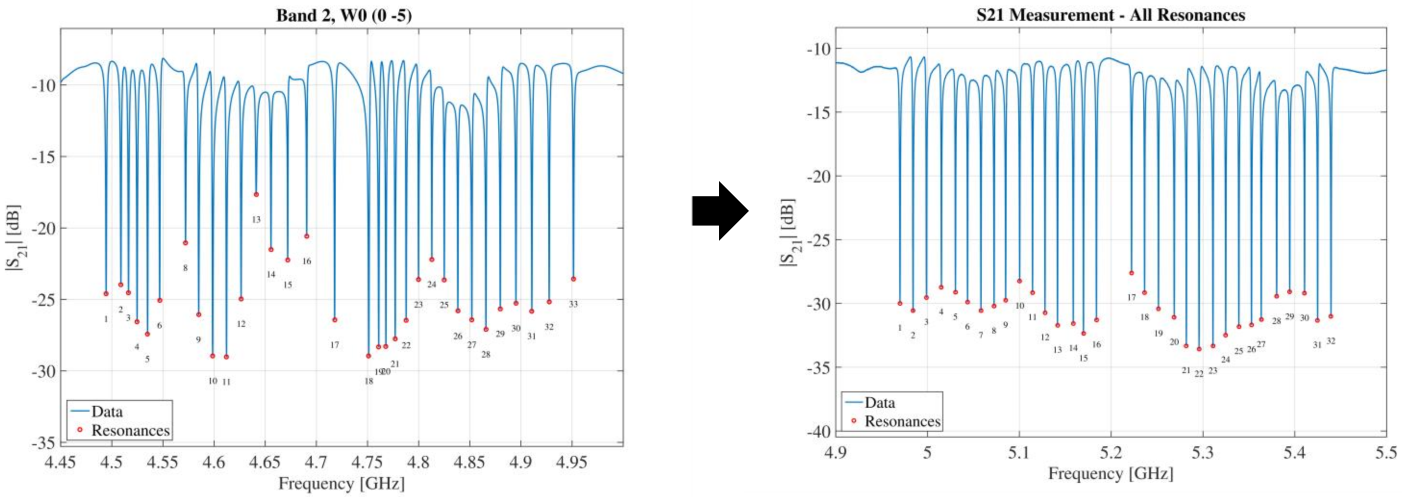

TES time profile

- RT and DT must be tuned to be as short as possible to minimize the fraction of pile-up and dead time, while keeping the single pixel activity high.

- With the current array (*HolmesKOHAu*), it is difficult to represent a distribution of RT that reflects the differences between the detectors

Example of the RT distribution in the *HolmesKOHAu* chip

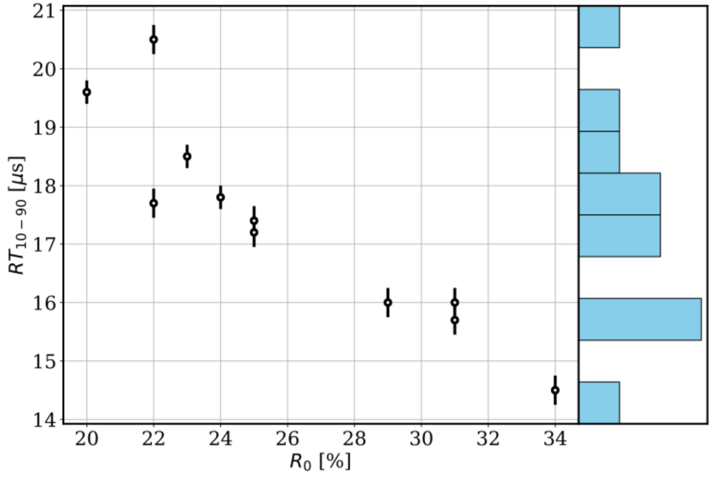

RT of the order of 20 μs, well suited for the Holmes goals.

The measured pulses were ~ 3 times slower than the ones entirely produced at NIST

- DT processed with KOH etching is not ideal.

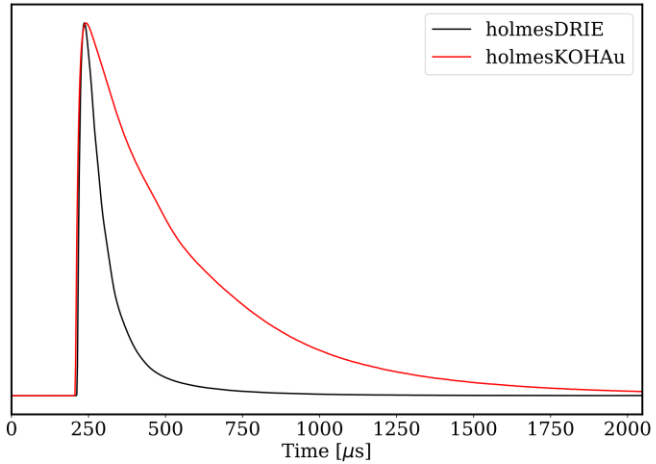

Something went wrong during the etching procedures?

TES time profile

- G was 25-50% lower than the target one ($\sim 600\ pW/K$)

Measured distribution of thermal conductance in *holmesKOHAu* chip

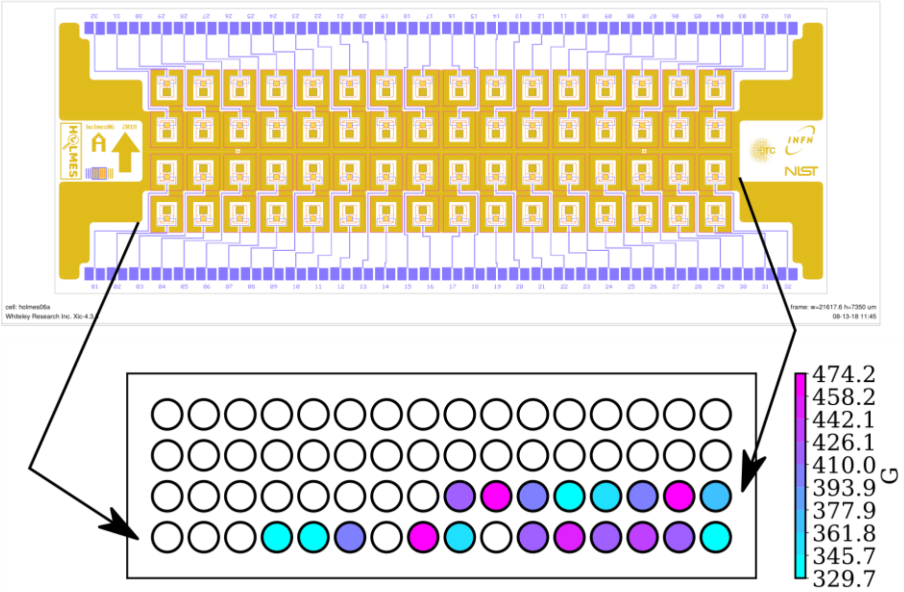

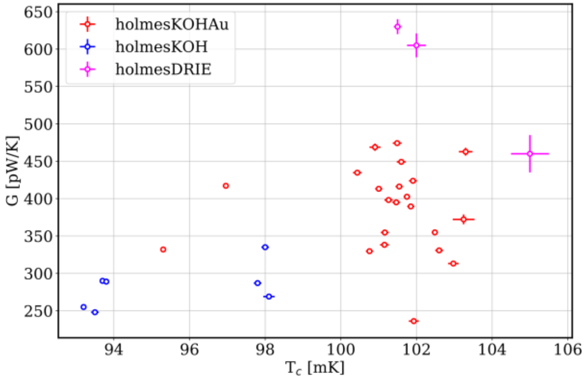

Distribution of (T, n, G) in the three chips studied

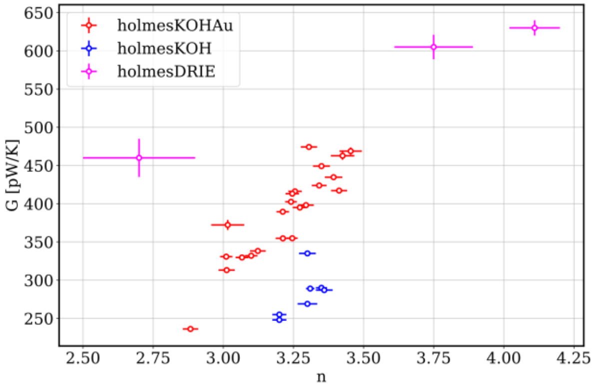

From IV curves to thermal conductance

$$P_{bath} = I_{TES}^2 R_{TES}$$ ← Measured with IV curves

$$= k(T_{TES}^n - T_{bath}^n)$$

$$= \frac{G T_{TES}}{n}\left[1 - \left(\frac{T_{bath}}{T_{TES}}\right)^n\right]$$

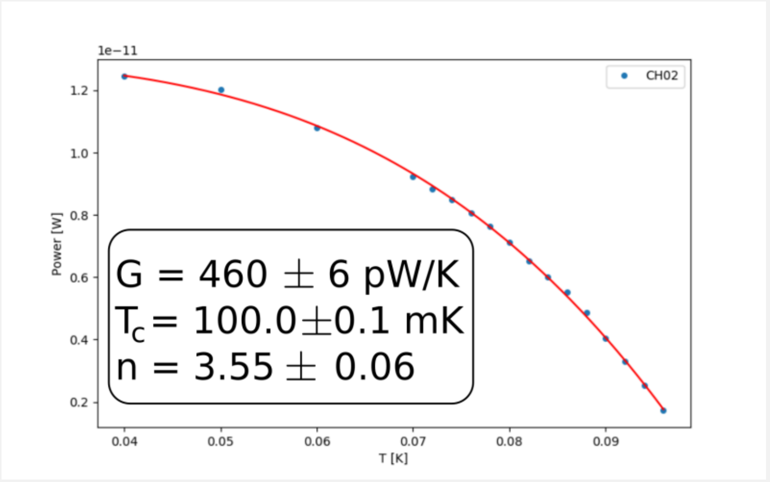

- Issue with the membrane/silicon production?
  - Diffusive phonon propagation due to the rough silicon surface

Noise spectrum

- Noise power spectrum of a single detector is given by: $n_{detetector} = n_{johnson,load} + n_{johnson,TES} + n_{TFN} + n_{SQUID}$ → $n_{SQUID} = n_{rf-SQUID} + n_{TLS} + \boldsymbol{n_{HEMT}}$

Acquired noise PSD for a pixel

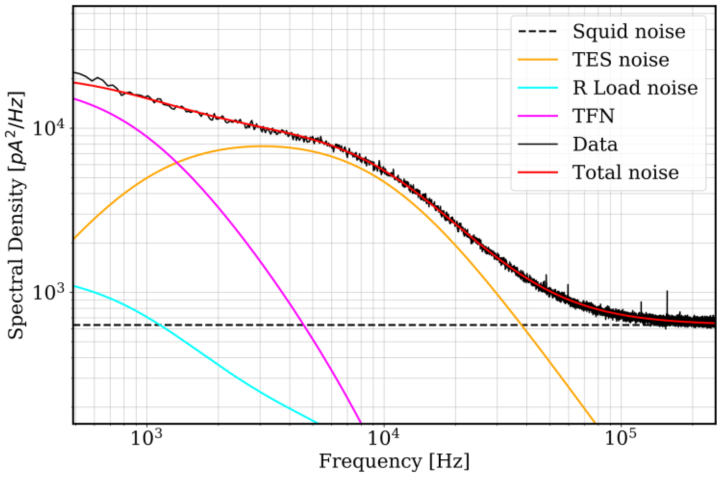

In reality, noise power spectrum is also affected by other contributions related to the microwave multiplexing technique.

IMD due to non-linear elements (DACs, μmux, HEMT…)

Increasing the number of detectors (tones) will also increase the strenght of these effects.

PSD of 32 unbiased TES

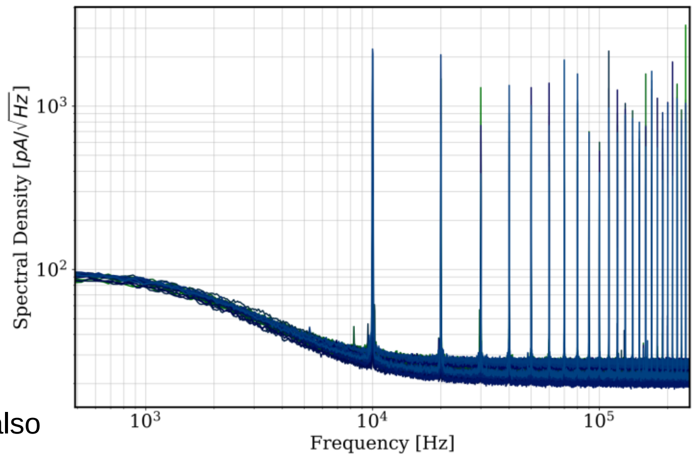

- Achieving a noise power spectrum which do not spoil the excellent intrinsic energy resolution of the detector requires **meticulous** attention during the probe tones setup.
- Our main obstacle seems to be related with the lowest frequency that the ROACH2 DDS can generate.
- The squid readout noise, including IMD, produce an optimal flat noise spectrum between 19-27 $\frac{pA}{\sqrt{Hz}}$

negligible impact on the energy resolution

First time multiplexing readout of 32 channels

PSD of 32 unbiased TES, no IMD

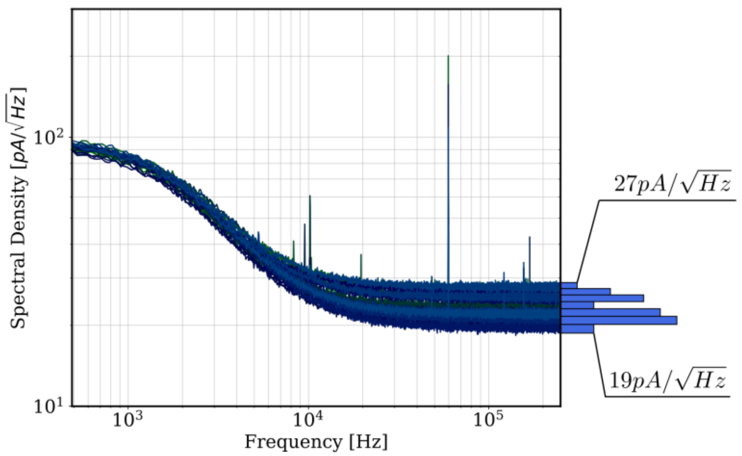

Same but with TES bias on

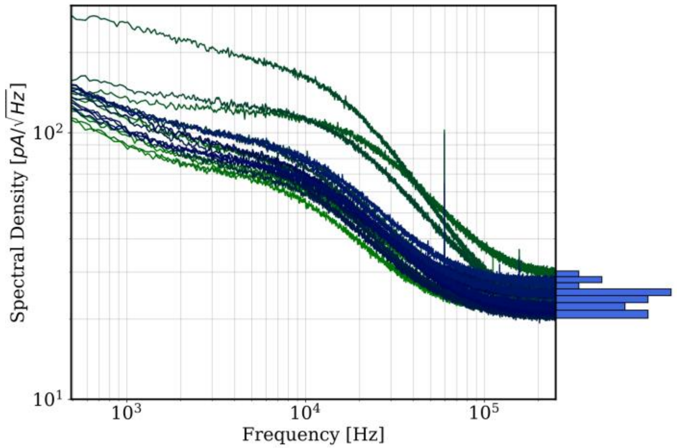

Energy resolution

- $\Delta E < 10$ eV : target energy resolution for activity of 300 Bq.
- More stringent energy resolution may be required in the first phase of Holmes to obtain meaningful results.

TES resolution for the Mn K_α line, *holmesDRIE*

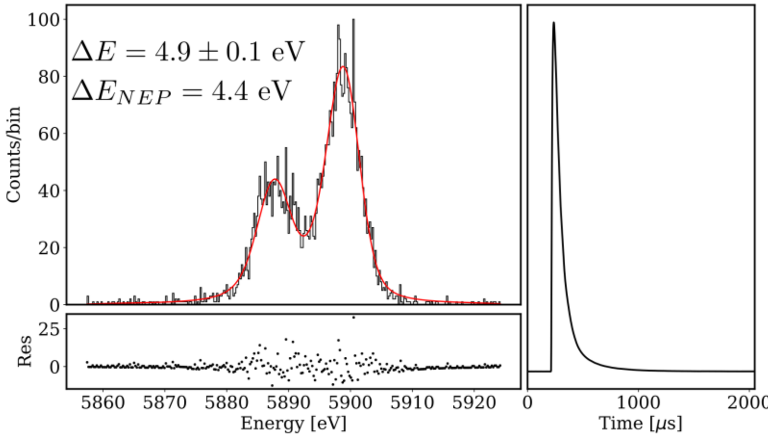

TES resolution for the Mn K_α line, *holmesKOH*

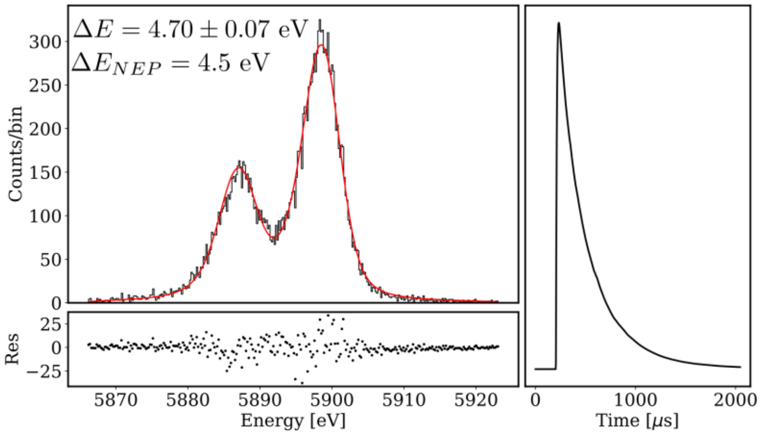

TES resolution for the Mn K_α line, *holmesKOHAu*

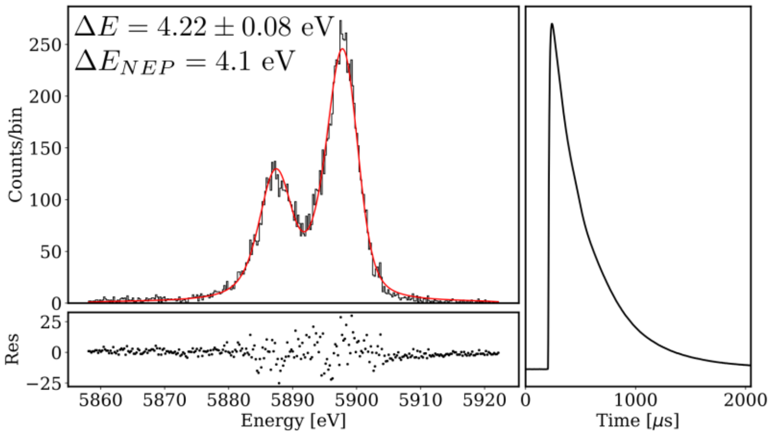

Energy resolution measured very close to the one predicted by the NEP (analysis routine are working).

The fabrication process did not spoil the TES performance in terms of energy resolution.

A further complication?

- For a Low Temperature Detector (LTD), the energy resolution and the detector time response is proportional to the detector heat capacity.
- Total detector heat capacity without Ho $C = C_{abs} + C_{sensor}$

e.g. Holmes TES $C_{abs} = 0.55\ pJ/K, C_{sensor} = 0.25\ pJ/K \rightarrow C \sim 0.8\ pJ/K$

Specific heat of bulk Ho metal

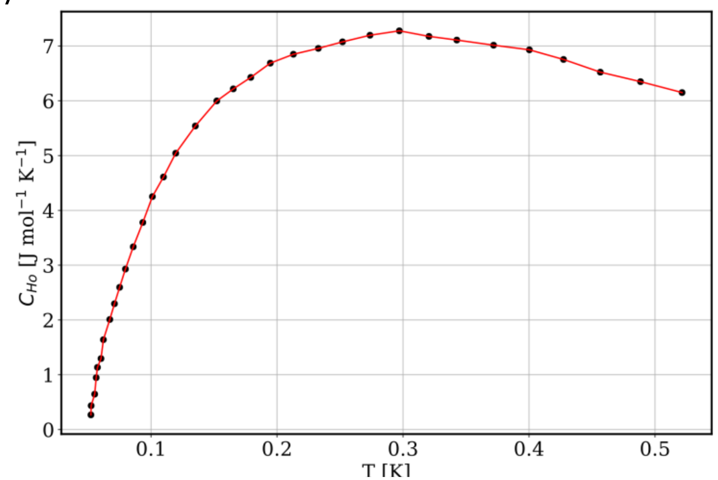

- Hyperfine interactions in rare-earth elements (Ho) causes a Schottky anomaly in the (C,T) plot.
- Total detector heat capacity with Ho $C = C_{abs,Au} + C_{sensor} + C_{abs,Ho}$
- Worst case scenario: the energy resolution could be worsen by a factor of 2 for an Ho activity of 1 Bq

Simulated signals with and without Ho

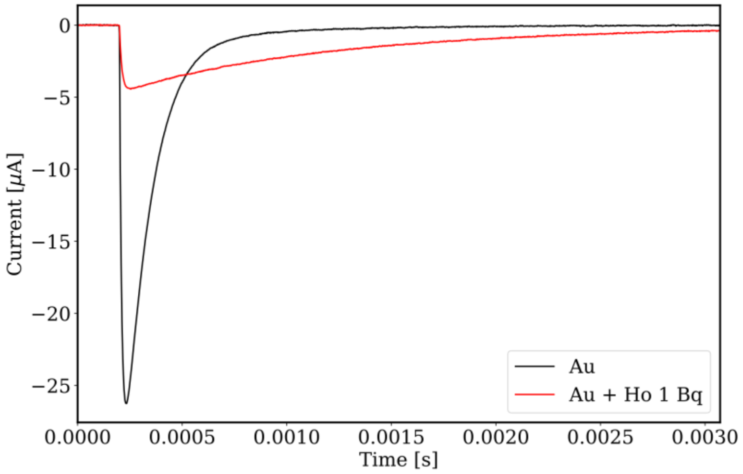

- $C_{abs,Ho}$ depends on
  - Implantation process
  - Absorber material
  - The chemical species of the implanted ^{163}Ho

Needs to be assessed for our implantation setup.

Background studies

- The count rate is particularly low in the region of the holmium spectrum near the end point ($0.26 \text{ counts eV}^{-1}\text{ day}^{-1}\text{det}^{-1}$ @ [2650,2833] eV)
- The fraction of background signals must be kept as low as possible.
- Background sources:

  - **Pile-up** → Pile-up will be the main background sources for activity per pixel 300 Bq. ($0.8 \text{ counts eV}^{-1}\text{ day}^{-1}\text{det}^{-1}$ @ [2650,2833] eV @ $\tau_R \sim 1.5\ \mu s$)
  - **Radionuclides in the detectors' absorber** → ^{166m}Ho (β decay, $Q_\beta = 1854$ keV, $\tau_{1/2} \sim 1200$ years). Expected count rate in the ROI $< 0.01 \text{ counts eV}^{-1}\text{ day}^{-1}\text{det}^{-1}$
  - **Natural radioactivity**
  - **Cosmic rays**

  → They can be comparable or even overcome the pile-up rate if the ^{163}Ho activity per pixel is too low.

Natural radioactivity and cosmic rays: MC

- Detectors approximated as cylinders of 0.226 mm diameter and 2 µm thickness above a holey Si substrate and inside a cylindrical copper holder.
- Radionuclides (^{238}U, ^{232}Th, ^{40}K, ^{210}Pb) places inside and on the surface of both the gold absorbers and the copper holder.
- Uniform «cosmic ray source» above the detector.

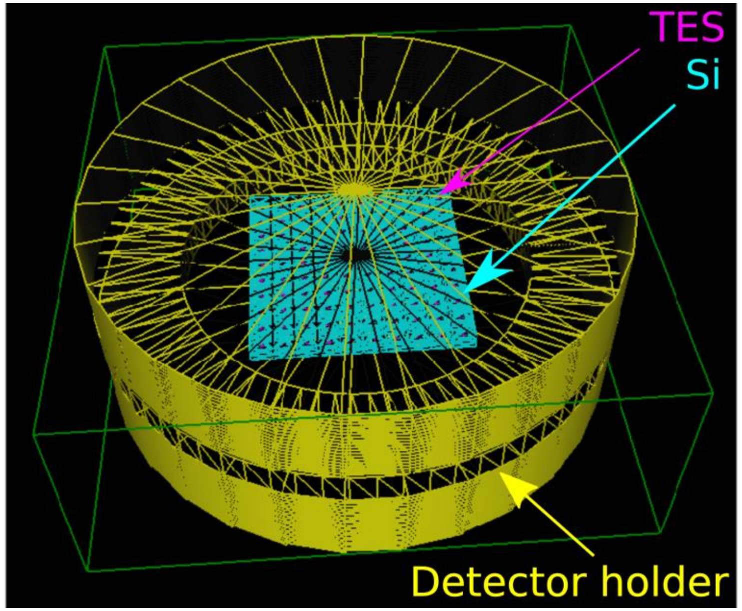

All **but** the ^{40}**K** produce a smooth and almost flat background in the ROI

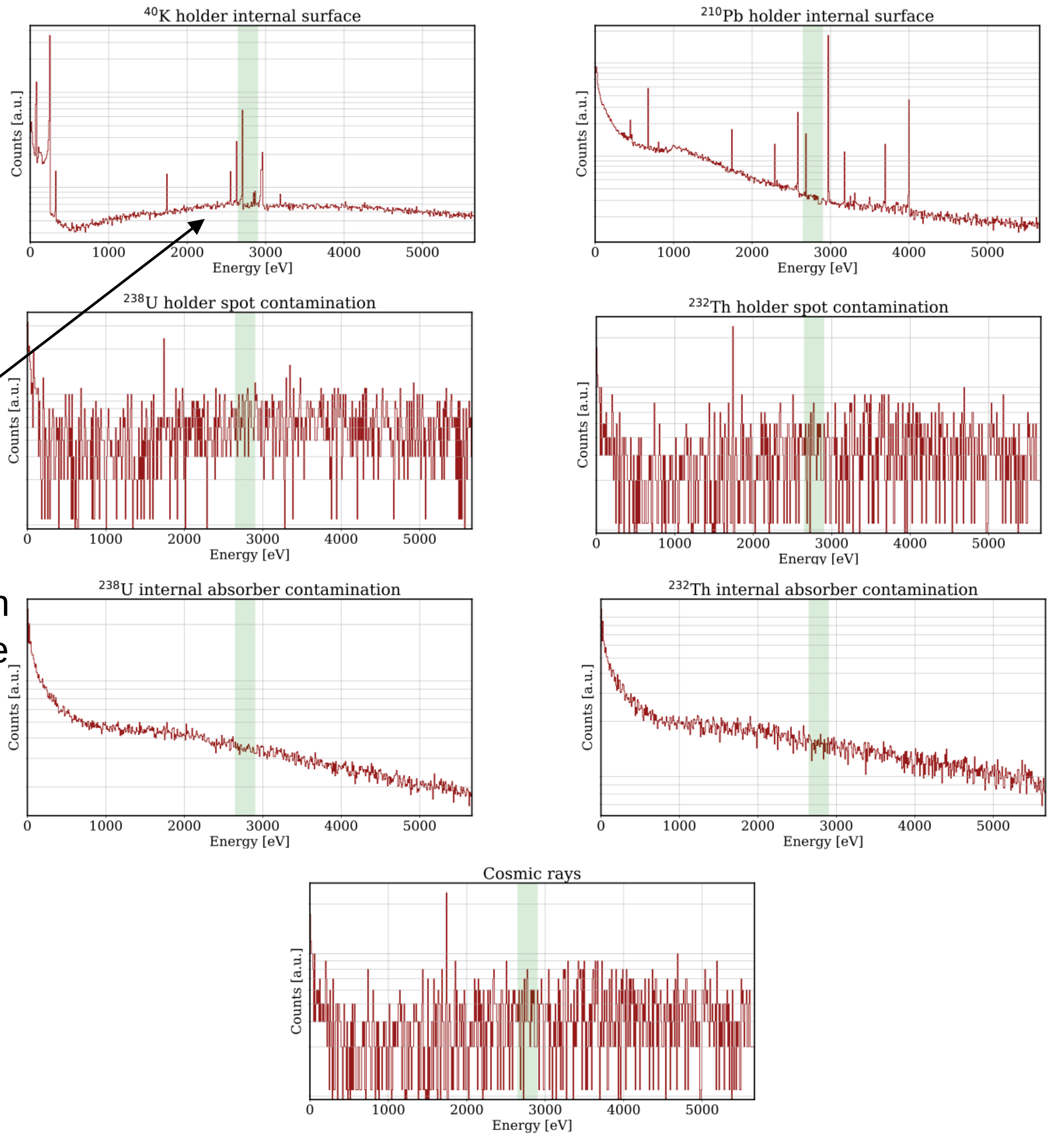

Natural radioactivity and cosmic rays: experimental setup

- Goal: estimate the background rate, determine the fraction due to CR, determine the impact of $^{40}\mathrm{K}$

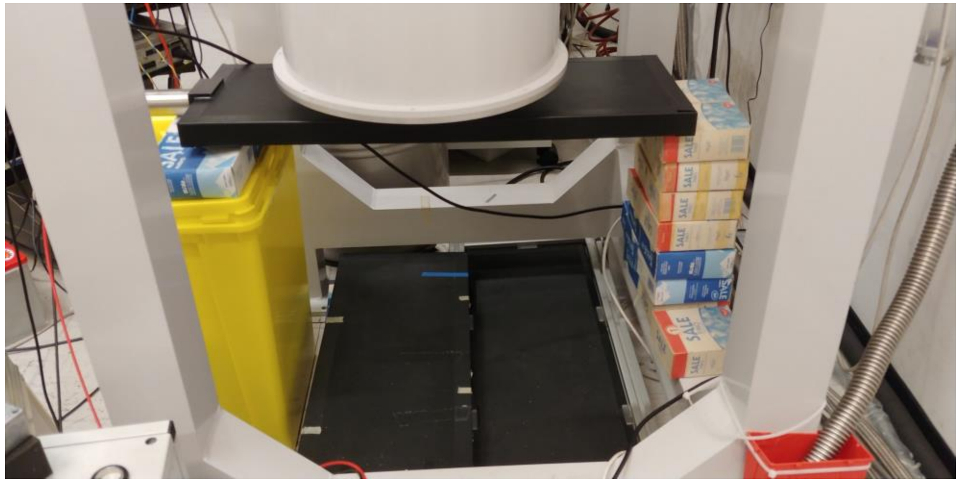

Experimental setup

- No calibration source
- Array of 32 detectors (different geometries)
  - 'Only' 16 detectors were measured.
- Three scintillators places under the cryostat
- Measurement done in August, lasted 500 hours

- With this scintillator setup we should measure the muons hitting the detectors with a geometrical efficiency of $\sim 50\%$

- Rate of scintillator coincidence signals ~ 7 Hz → cosmic rays vertical flux $I \sim 0.2 cm^{-2} min^{-1}$

  In agreement with an overburden mass $m_{ob} \sim 18$ mwe, measured in previous studies

- Syncing an external signal with the output signals from the detectors array is not trivial, due to the microwave multiplexing technique.

  We exploited the presence of the dark squid.

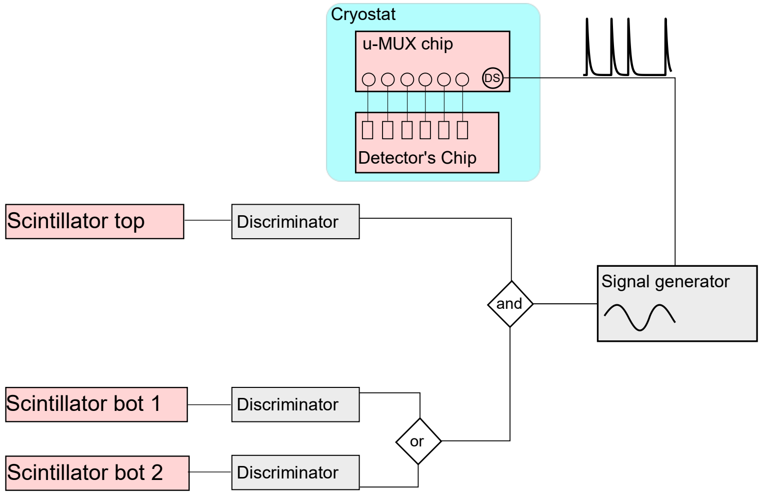

Natural radioactivity and cosmic rays: detector calibration

- Detectors not previously characterized ⊕ different geometries ⊕ no calibration sources ⊕ no statistically significant peaks expected @ [0,10] keV

  Dauting problem.

- To solve this, several approximations are necessary:

$$C\frac{dT}{dt} = P_J - P_{bath} + P$$

$$I(t) = -1 \times k_{\Phi_0/A} \times s(t) + I_0$$

$$P_J = I(t)^2 R_{TES} \cong (R_0 + R_L) I(t)^2 - R_L I(t)^2$$

$$E = \int P_{bath}(t)dt + \int P_j(t)dt$$

$$P_{bath}(t) \cong P_{bath,0} = R_0 I_0^2 = cost$$

$$E \cong E^* = \int_{t_0}^{t_f} R_0 I_0^2 dt - \int_{t_0}^{t_f} R_0 I(t)^2 dt$$

$$E^*_{cor} \equiv p_1 + p_2 E^* + p_3 (E^*)^2$$

Trend of the E^* parameter compared with the true simulated energy

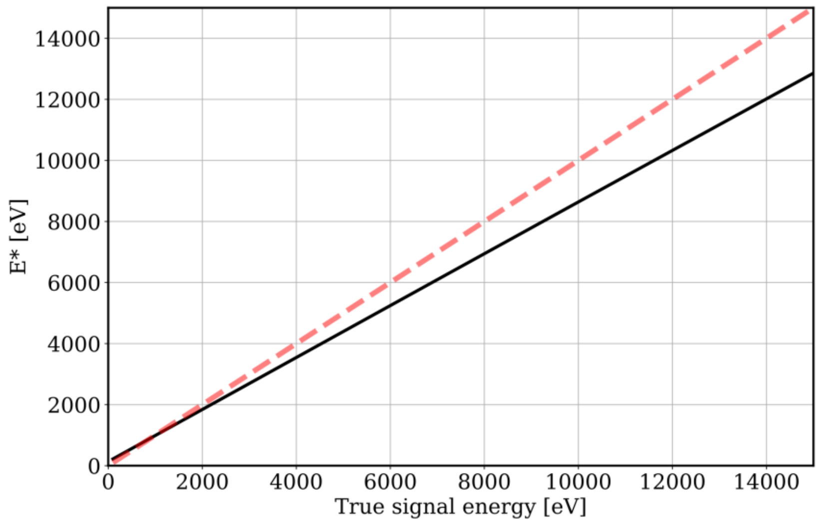

E^{cal} [eV]	E^* [eV]	E^*_{cor} [eV]
1455	1300 ± 260	1369 ± 273
3655	2930 ± 586	3278 ± 655
5898	4635 ± 927	5278 ± 1055

- This procedure can not be used to a precise energy determination of the signals, **but** it can be used for an estimation of the number of events inside a sufficiently wide energy interval.

Natural radioactivity and cosmic rays: Expected background rate

- The signals were tagged as single interaction, TES-TES or TES-scintillator coincidences
- After calibration, the data from each detector was merged to produce three different spectrum for each tag
- The TES-TES background spectrum is composed of radiation that directly hits multiple absorbers or that interacts with the materials between the pixels.

About the data analysis

- To estimate the background rate in each energy interval, a Bayesian learning procedure was adopted to update the posterior distribution

  Probability distribution for the rate r in the i-th bin = $P(r|N,c) \propto r^c e^{-cN}$ (rate)

  $$c = \sum_{j=1}^{N} x_j$$

  N → Number of detectors; x_j → Counts of the j-th detector in that bin
- The data points in each plot represents the expected background rate in each bin, expressed as mean value of the gamma distribution.
- The errors bars are the 95% credibility intervals, evaluated symmetrically from the median.
- For zero counts, the errors represents the 95% upper limits

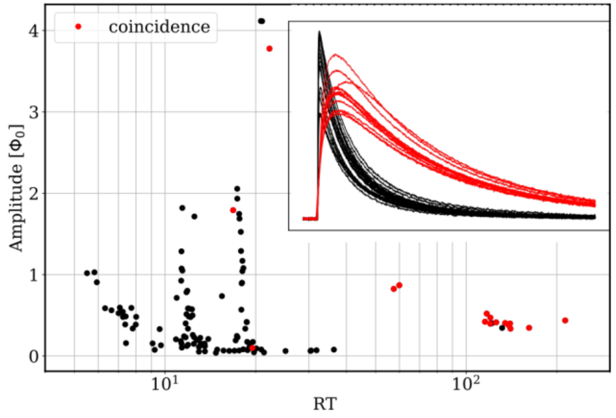

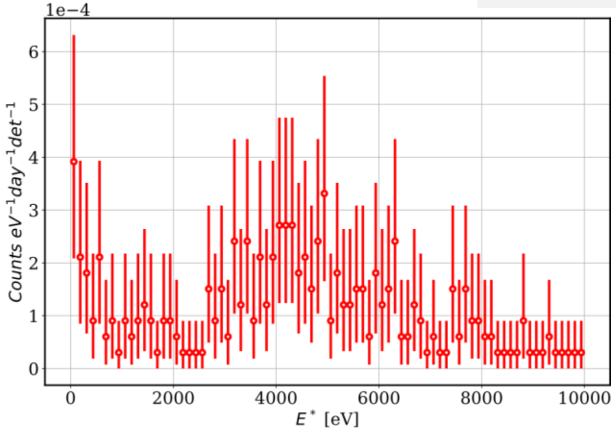

➡ These signals **do not** contribute to the final background rate.

- The **TES-scintillator background spectrum could not be used** to study the muon-induced background rate. → **Timestamp problem**, tagging efficiency too low -> only *O*(10) events out of ~ 1500 were recognized as muon induced.

Natural radioactivity and cosmic rays: Expected background rate

- Single interaction produce a background spectrum which seems to be monotonically decreasing. Background rate in the ROI

$0.5 \times 10^{-3}\ \mathrm{counts\ eV^{-1}\ day^{-1} det^{-1}}$

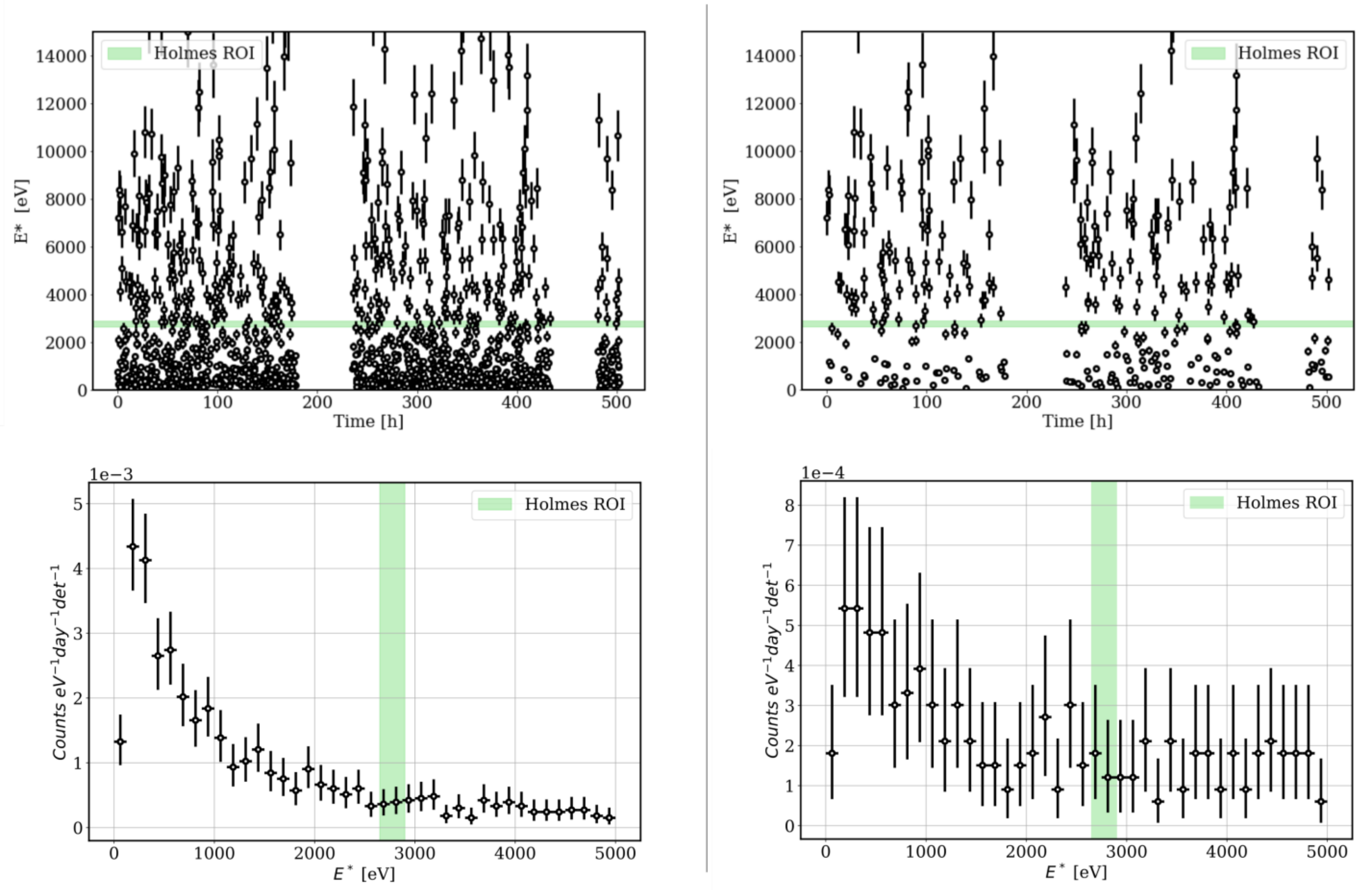

With simple cut on the signal shape

$1 \times 10^{-4}\ \mathrm{counts\ eV^{-1}\ day^{-1} det^{-1}}$

- Second level data reduction and most conservative cut will further improve this results in practice.

Natural radioactivity and cosmic rays: muon induced events

- The TES-scintillator background spectrum could not be used to study the muon-induced background rate.
- We had to follow a different procedure, based on MC simulations, just to have an idea of the order of magnitude of the fraction of background rate which is muon induced, f_μ
  - The data were divided in equal time interval lasting 5 hours

$$c_i = Poisson(c_i | N_i^\mu + N^b)$$

Mean number of muon induced events

Total counts recorded by the array in the i-th interval

Mean number of events due to radioactivity

$$N_i^\mu = k \times N_i^s$$

$$k = P(A|B) = P(B|A)\frac{P(A)}{P(B)}$$

Probability that a muon induced events hits the array

Evaluated from the MC simulations

Probability that a muon induced events hits the top and bottom plane of the scintillators

$$\alpha = \arctan r_{top}/d_{bs}$$

$$P(B|A) = \frac{\int_0^\alpha \cos(\theta)^2 \, d\theta}{\int_0^{\frac{\pi}{2}} \cos(\theta)^2 \, d\theta} \qquad P(B) = \frac{\int_0^\beta \cos(\theta)^2 \, d\theta}{\int_0^{\frac{\pi}{2}} \cos(\theta)^2 \, d\theta}$$

$$\beta = \arctan r_{bot}/d_{ss}$$

$$\cong 0.5 \frac{2.97 \times 10^{-5}}{0.86} = 1.75 \times 10^{-5}$$

$$f_\mu = < f_\mu > = 1 - \frac{N \times N_b}{\sum c_i}$$

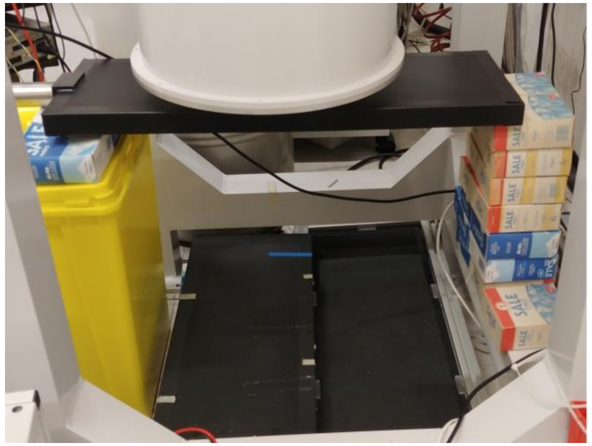

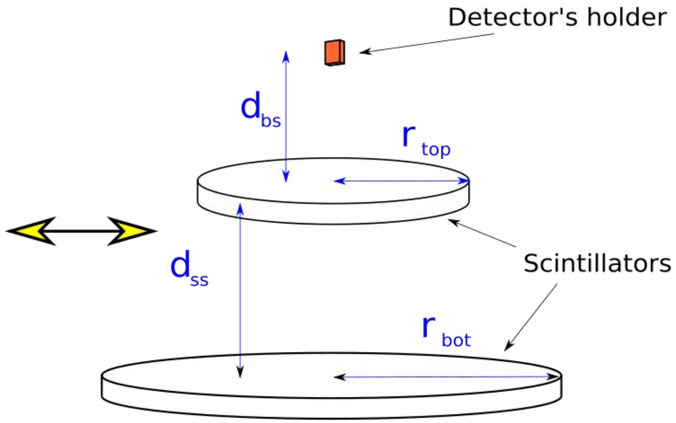

- The fraction of muon induced events was measured having a mean value of $E[f_\mu] = 0.460 \pm 0.002$, with a plausible interval of 90% between [0.28,0.59]

Natural radioactivity and cosmic rays: K and expected neutrino mass sensitivity

- Both the gamma and the electron from the beta decay produce a flat spectrum in the ROI region, while the EC produces de-excitation peaks with energy into and close to the ROI.
- If those peaks are present but not modelled in the final spectrum, they could potentially worsen the experimental sensitivity.
- We have studied qualitatively how a posterior of the neutrino mass changed if the likelihood did not include the $^{40}\mathrm{K}$ peaks by varying the number of counts *B* under those peaks.

Toy MC info

- Number of detectors = 32, $\Delta E = 5\ eV, \tau_R = 1.5\ \mu s$
- Measurement time = 3 years
- First order Ho spectrum
- Bkg rate = 5×10^{-5} counts $\mathrm{eV}^{-1}\,\mathrm{day}^{-1}\mathrm{det}^{-1}$

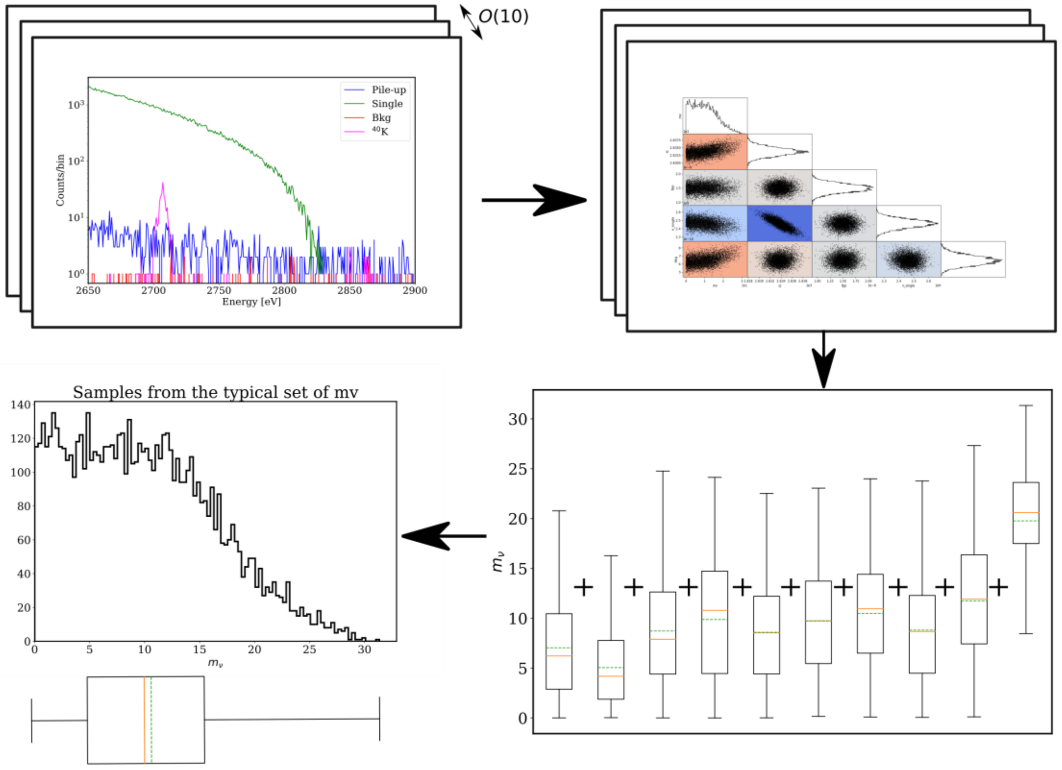

- Normal priors for Q, f_{pp}, bkg and n_{single}, while for m_ν a slightly uninformative exponential distribution

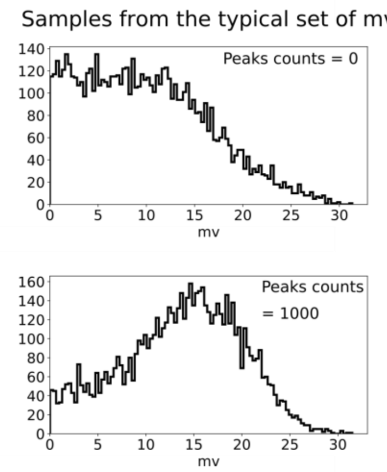

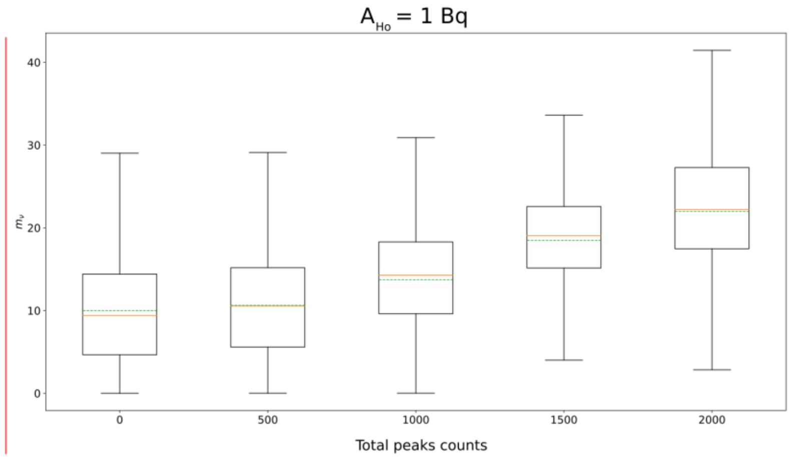

- MC simulation were used to convert *B* to a surface density of K on the holder cover

$$B = 1000 \leftrightarrow 0.5 \frac{mg}{cm^2} \text{ of K}$$

Preliminary conclusion: influence of $^{40}\mathrm{K}$ on the neutrino mass sensitivity will be negligible.

Pile-up rejection

- The pile-up fraction f_{pp} is proportional to the time resolution τ_R. The latter depends on the detector and readout characteristics and on the algorithms used to discriminate the signals.
- Requirements: high discrimination efficiency and **near zero energy dependence**.
- We have studied an application of the Wiener Filter while developing a new discrimination technique called DSVP.
- To test the algorithm, we wrote a tool to simulate the detector response (signal shape and noise spectrum.

Simulation program in a nutshell:

- Goal: create pseudo-real dataset
- Energy taken from the first order Ho spectrum
- 4-th order Runge-Kutta method to solve the *n* differential equations
- ARMA(p,q) to properly simulate the noise spectrum

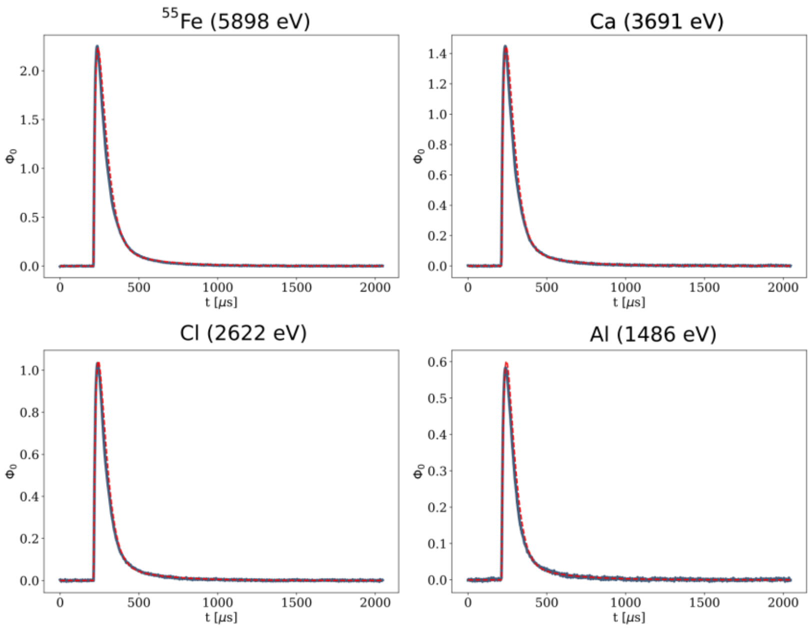

Real pulse **Simulated pulse**

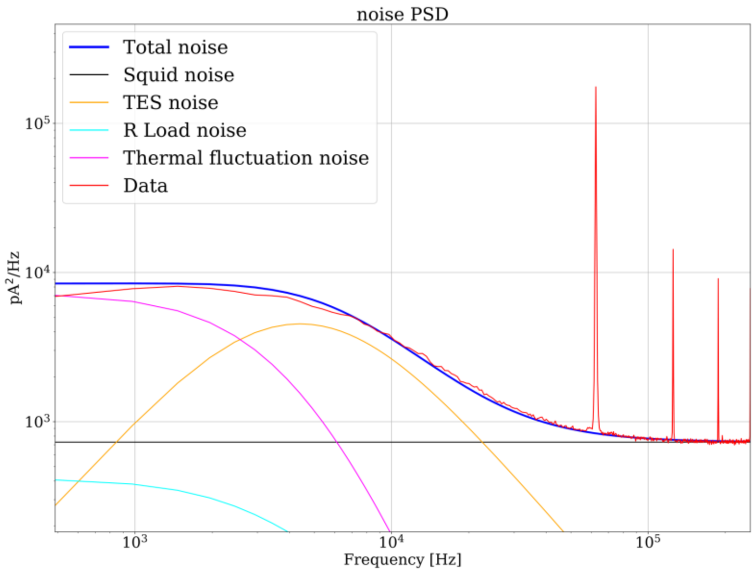

Simulated pulse profile of non-linear vs linear detector

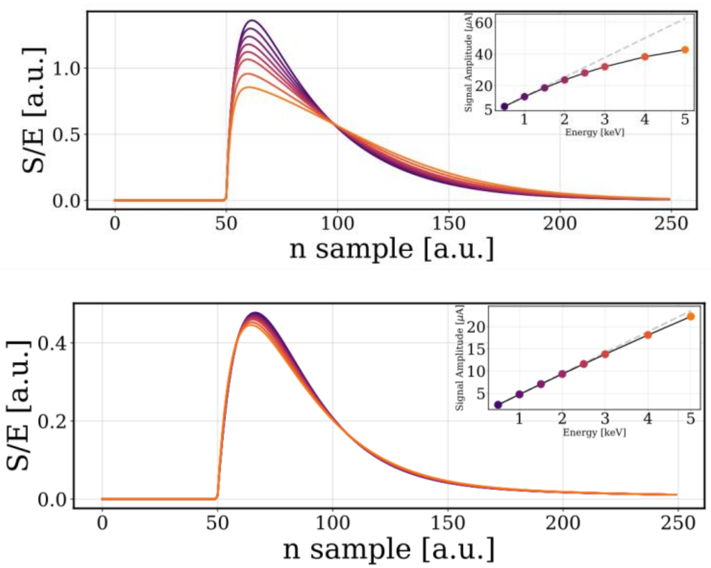

Lowering the pile-up fraction

- Two dataset were simulated:
  - *Full spectrum*: full Ho spectrum, $A = 300\ Bq, T_{meas} = 1\ h \rightarrow 7 \times 10^5$ events recorded (61% single pulses, 31% double, 6% triple…)
  - *ROI*: $\mathrm{T_{meas}} = 2\ \mathrm{y},\ \tau_R \sim 10\ \mu s\ , A = 300\ Bq, \mathrm{E}\ \in [2650{,}2900]\ eV \rightarrow 4 \times 10^4$ single pulses and 8×10^4 pile-up pulses

- To test the algorithm effectiveness, three different detector response were simulated:

  (a) Detector with a strongly non-linear response and one thermal body
  (b) Target detector of Holmes, nearly-linear response and two body model
  (c) Detector close to the one in the *holmesKOH* arrays

- To quantify the efficiency of the different strategies, an effective time resolution was defined:

$$\tau_{eff} = \left(\frac{\#\ pileup}{\#single}\right)_{final} \times \left(\frac{\#single}{\#pileup}\right)_{initial} \times \delta t$$

- To apply the DSVP, the f_{pp} in the ROI must be first reduced below 1.

  Two different strategies were investigated:
  1. Wiener filter
  2. Adding an external calibration source

Lowering the pile-up fraction

- With the target detector of HOLMES, the DSVP (+ Wiener Filter / Pd source) technique allows to reduce the $f_{pp}$from 10^{-3}($\sim \tau_{eff}$ $3\ \mu s$) to 10^{-4}($\sim \tau_{eff}$ $1.5\ \mu s$)

Detector type	Rise time [μs]	t_{sample} [μs]	τ_{eff} [μs] (WF)	τ_{eff} [μs] (DSVP)
(b)	11	2	2.26	1.55
(b)	17	2	2.37	1.55
(b)	22	2	2.94	2.01
(b)	17	1	1.66	0.94
(a)	10	2	1.82	1.24
(c)	19	2	2.70	1.82

Borghesi, M., et al. "A novel approach for nearly-coincident events rejection" EPJC

Time resolution lower than the sampling time!

ROI energy spectrum

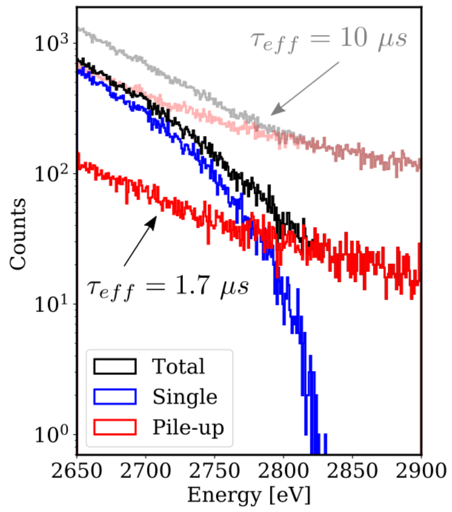

The dependance of τ_{eff} and the average percentage of false positive (*F*+) from the input parameter

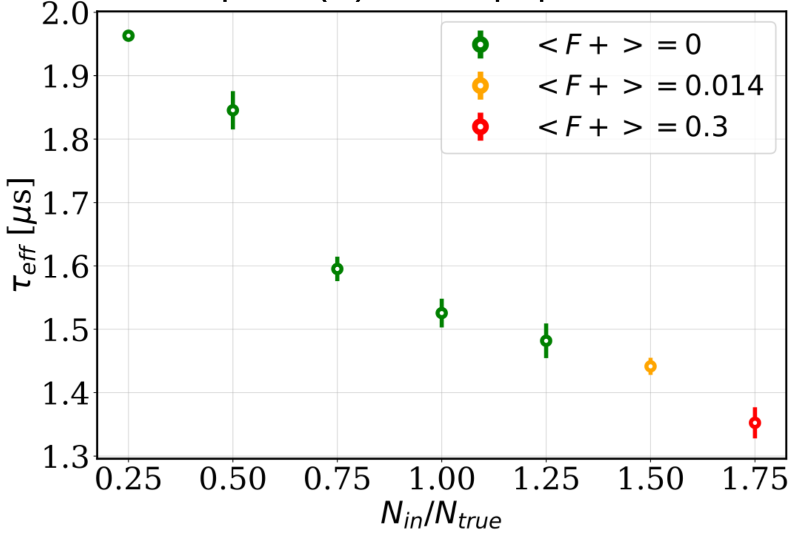

ROI energy spectrum with Pd source

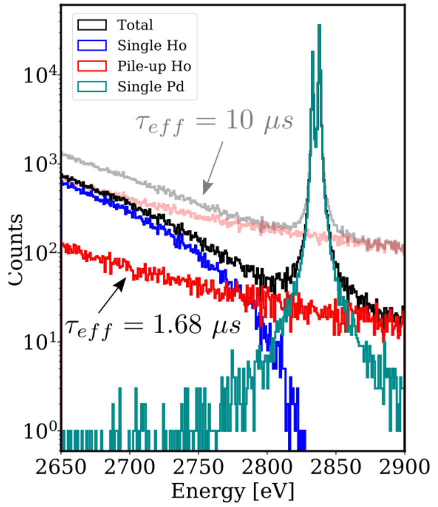

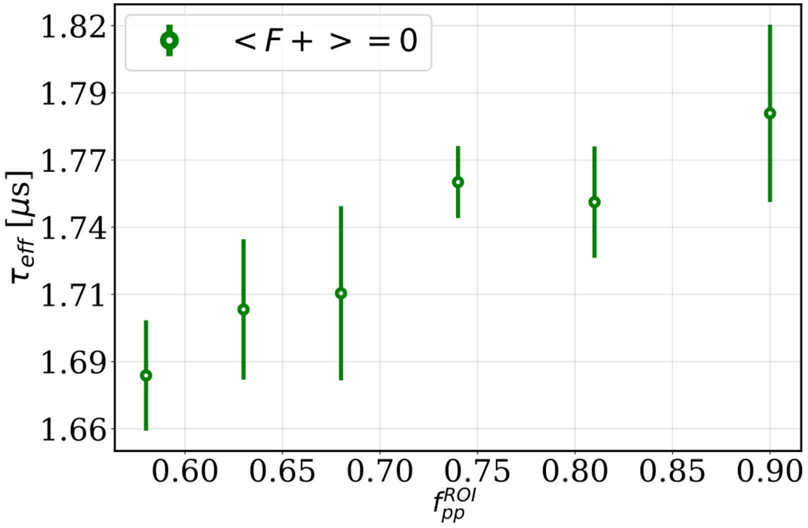

Conclusions

- Tested and tuned the final array fabrication processes.
  - These did not spoil the detectors' performances.

- The software for analysis and signal processing of microcalorimeters events is up and running!

- The expected background contributions were assessed, both with simulations and dedicate measurements.
  - A further reduction of a factor roughly 25% could be achieved with a similar setup studied in this work (muon veto).
  - Pile-up reduction results equivalent to increase the measurement time by a factor 4: from 3 to 12 years.

- Ion implanter is working as expected. The production of a proper sputter target is almost ready!

- The first phase of the HOLMES experiment is expected on the last quarter of 2022: a low dose implantation of a 2×32 pixel array.
  - Influence of the Ho on the detector response will be assessed
  - A high resolution Ho calorimetric spectrum will help to discriminate between the different theoretical models
  - A first limit on the neutrino mass $O(10)$ eV will be reached

- These results will contribute to clarify if the calorimetric approach can still be considered a feasible way to reach the required sub-eV sensitivity on the neutrino mass.

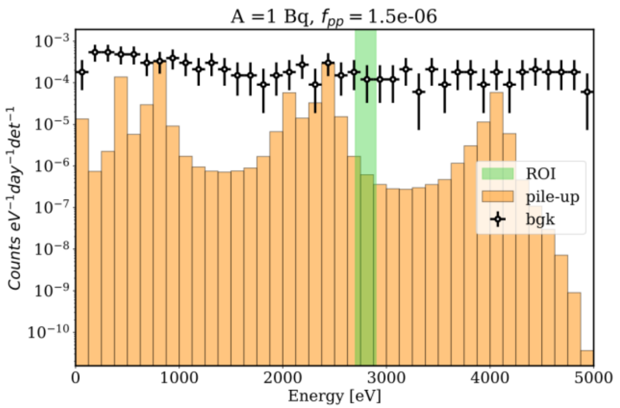

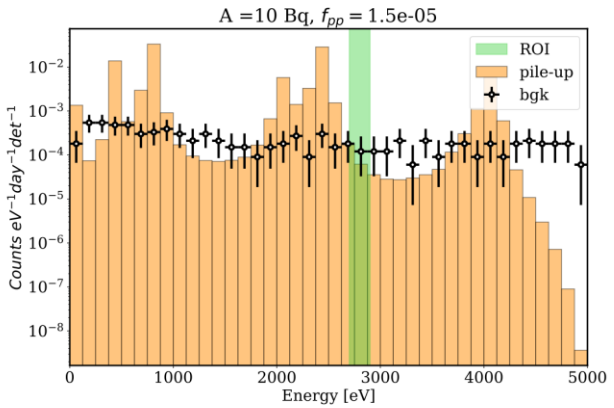

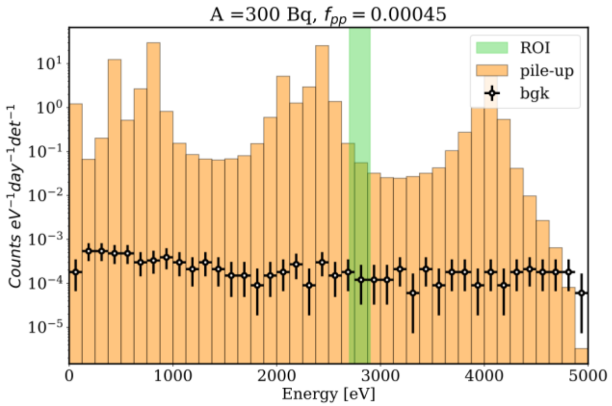

BACKUP

Natural radioactivity and cosmic rays: Expected background rate

- Single interaction produce a background spectrum which seems to be monotonically decreasing. Background rate in the ROI

0.5×10^{-3} counts $\mathrm{eV}^{-1}\,\mathrm{day}^{-1}\mathrm{det}^{-1}$…

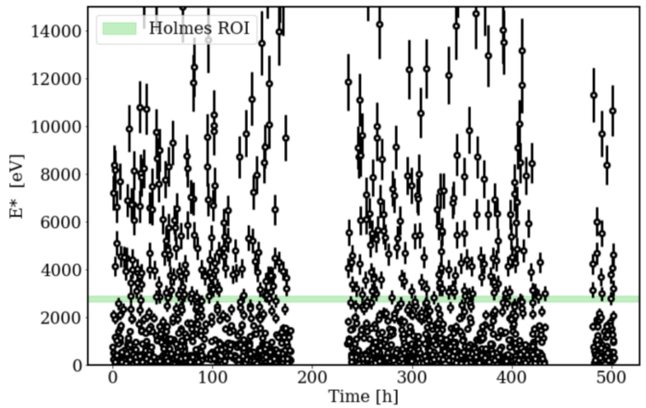

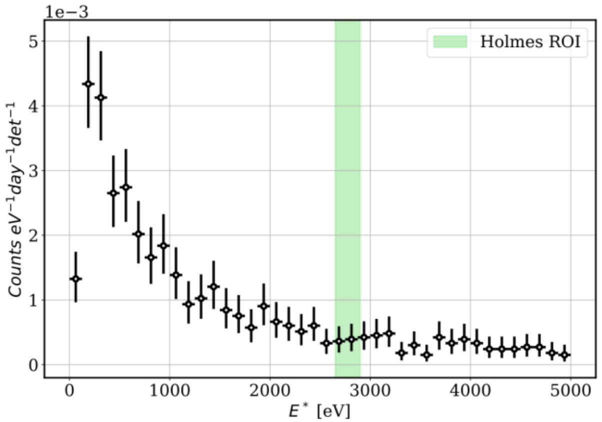

… but it is reasonable to believe **that a great fraction of events are radiations which do not interact directly with the absorber** (detector surroundings, copper perimeter, thermometer itself..)

Different signal shape

Old measurement with X ray calibration source on

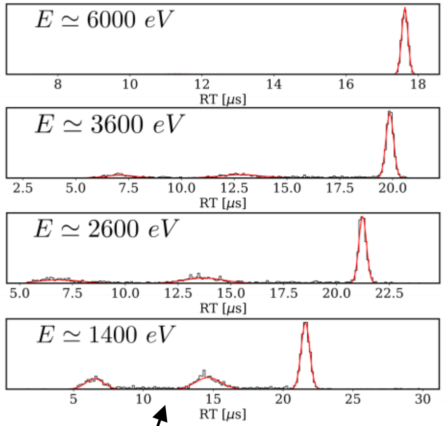

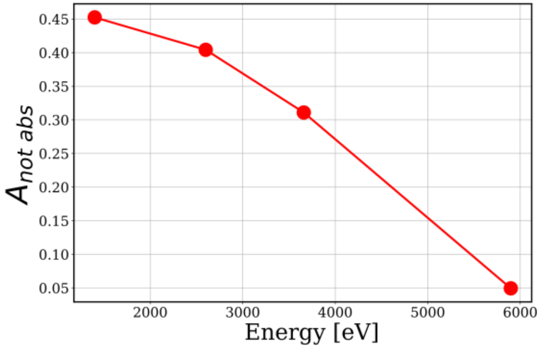

- The exact location of the RT band should be known.

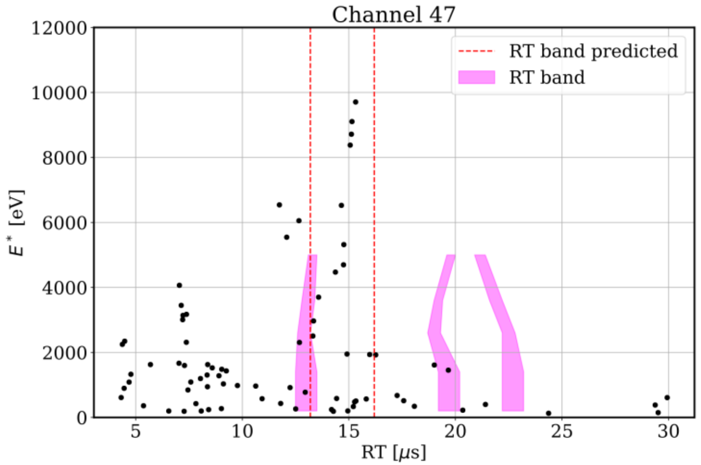

- The location of the RT band for the interaction in the absorber (i.e. for true Ho decays), can be estimated by looking at the RT of high energy events ($E > 6$ keV).

Data type and dead time

- Each recorded window (event) is composed of *N* samples

$$N = N_{base} + N_{pulse}$$

Example: detector decay time (DT) $70\ \mu s \rightarrow N = 1024$

$400\ \mu s \rightarrow N = 1536$

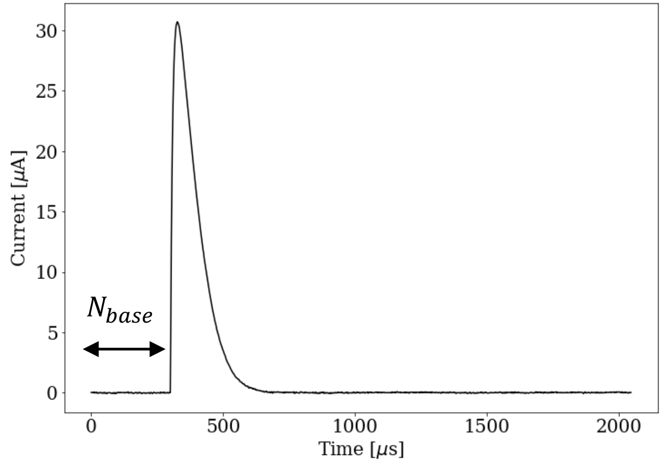

- It is possible to categorize the acquired signals into three main classes:

Clean events: One pulse + constant baseline

Multiple events: Two or more distinguishable pulses

Dirt events: $\geq$ 1 pulse + non constant baseline

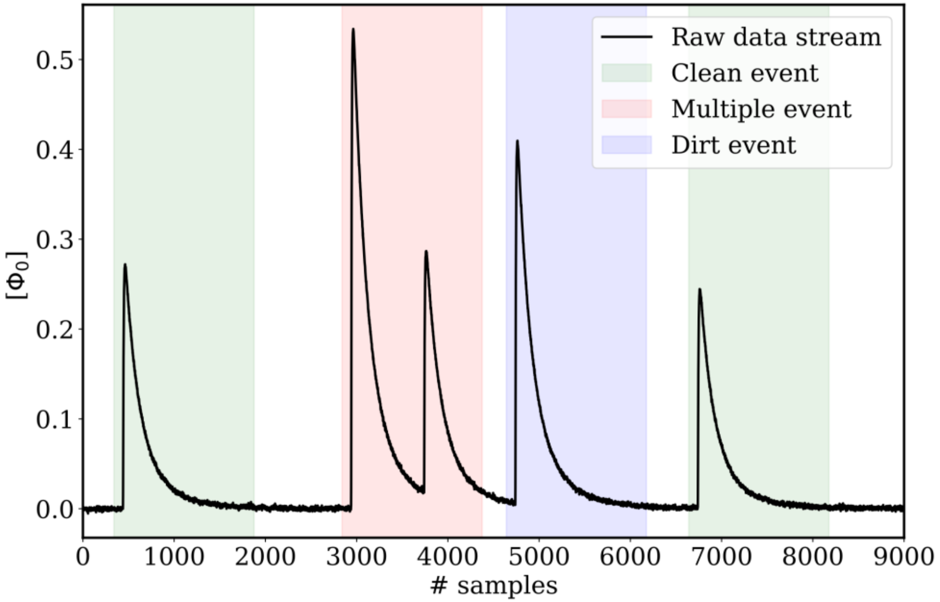

Detector activity	N	Dead time [%]	$\%\Sigma\ m_\nu$
1	1024	0.2	0.06
	1536	0.4	0.2
10	1024	2	0.6
	1536	4	2
300	1024	49	16
	1536	72	28

Fast signal correction

- Remember: with microwave multiplexing readout, the samples of the signals are **phase shift** whose value is proportional to the detector's current.

- The data must be unwrapped before being stored.

- If the current slew rate of a pulse is too high, the unwrapping algorithm will fail. This produce a so called *fast signal.*

  Probability of a fast signal:
  - Detector and readout properties
  - Time difference between energy deposition and first recorded sample
  - **Energy of the event**

- Fast signals distort energy spectrum

  ↓

  their correction is mandatory.

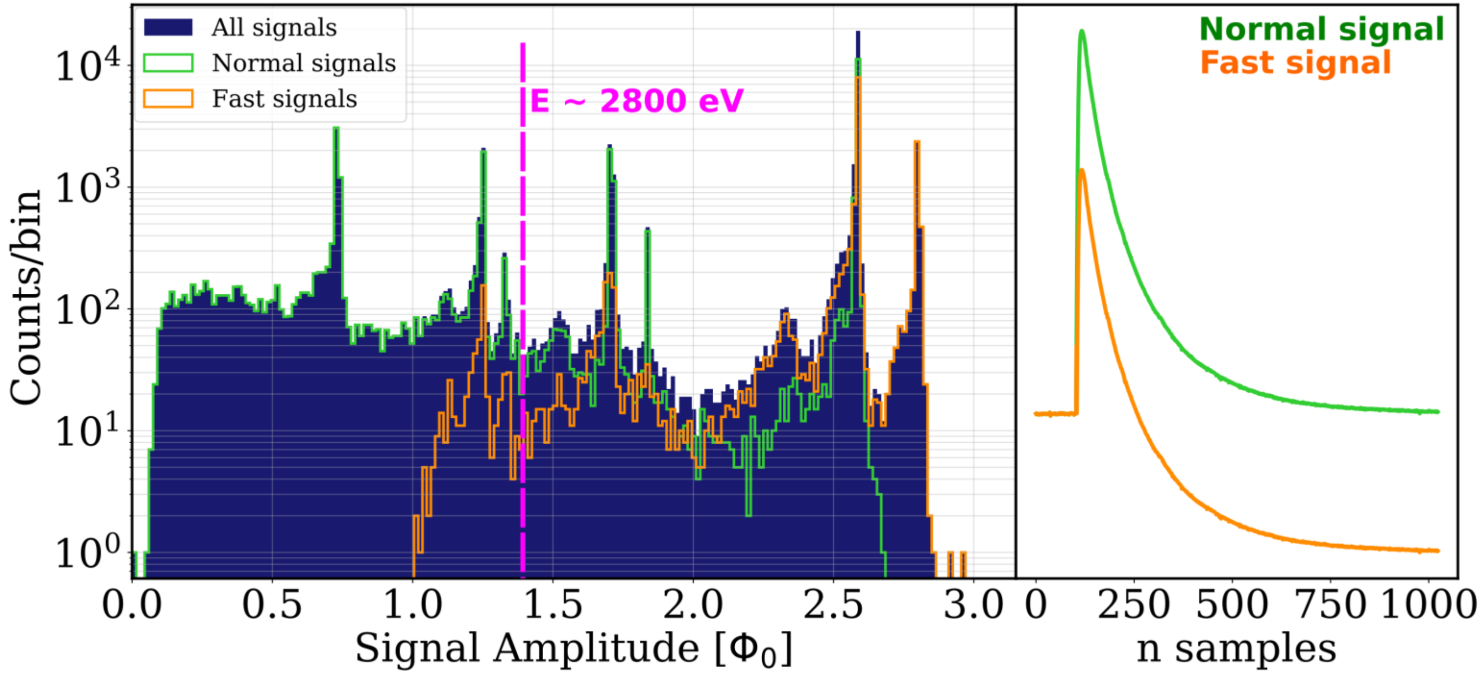

From raw data to 'clean' calibrated spectrum

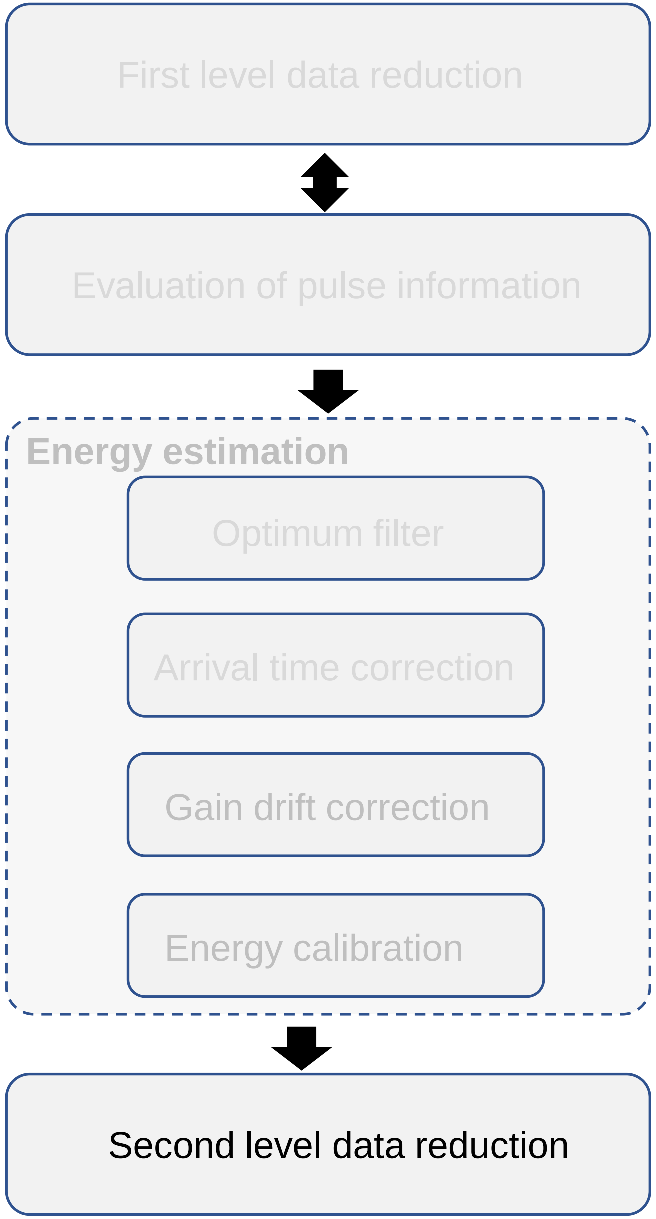

- Advanced discrimination techniques to further clean the dataset (pile-up events!)

Discrimination through Singular Vector Projections (DSVP)

- Novel "unsupervised learning" technique, based on singular value decomposition, PCA and multiple linear regression to identify as many undesirable events as possible from a dataset.
- The dataset need to have more clean events than unclean ones.

Dimensional reduction
Raw dataset cleaning (PCA)
Model the points distribution (Taylor expansion + weighted linear regression)
Define a threshold to cut

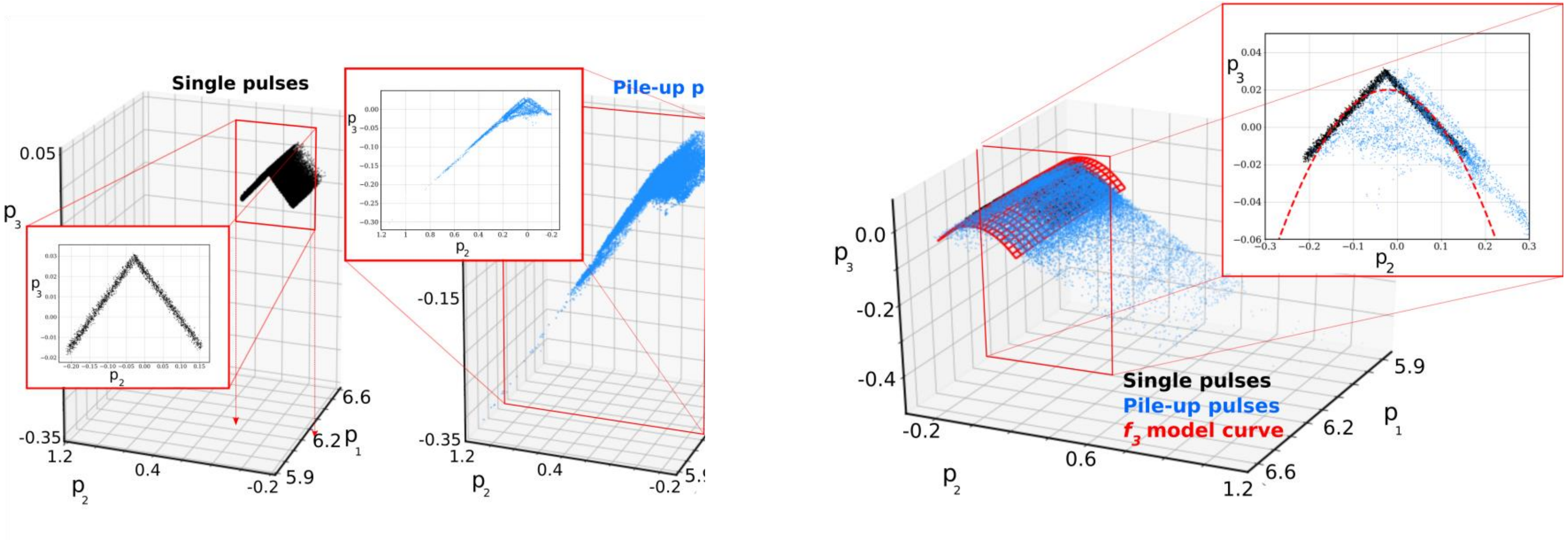

Lowering the pile-up fraction: DSVP and Wiener Filter

- The wiener filter (WF) transfer function is evaluated with a dataset containing roughly monoenergetic single pulses (the pulses from the M1 peak)
  - The WF is then applied both @M1 and @ROI. For each pulse, the three WF parameters ($WF_w, WF_{pts}, WF_{delay}$) are evaluated
  - WF_w presents a energy dependency, how to make a proper cut @ROI?

$$WF_w^{min,max}(ROI) = WF_W^{min,max}(M1) + \Delta x$$

  - After the WF cuts, the f_{pp} is finally below 1.

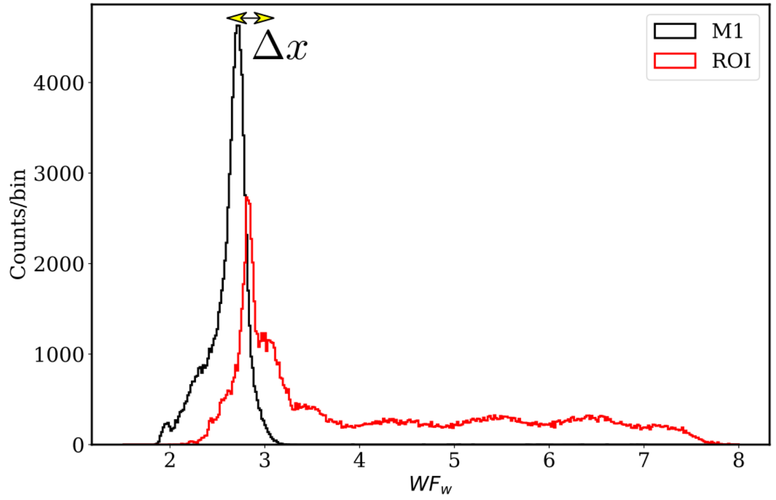

- Apply the DSVP on the resulting ROI dataset.

  Effect of a bad choice of N_{in} was investigated.

  No false positive was detected, even if we get the number of events to eliminate wrong up to 50%

Time resolution lower than the sampling time!

ROI energy spectrum

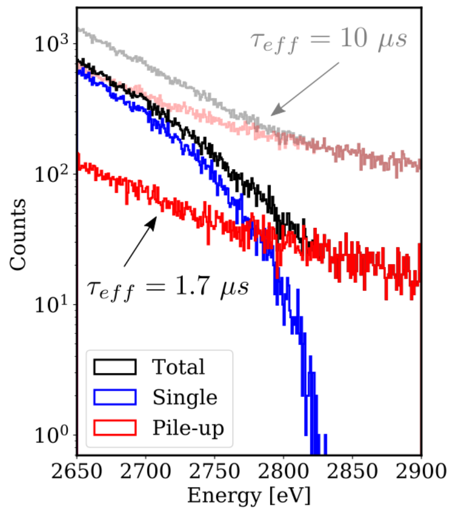

The dependance of τ_{eff} and the average percentage of false positive (*F*+) from the input parameter

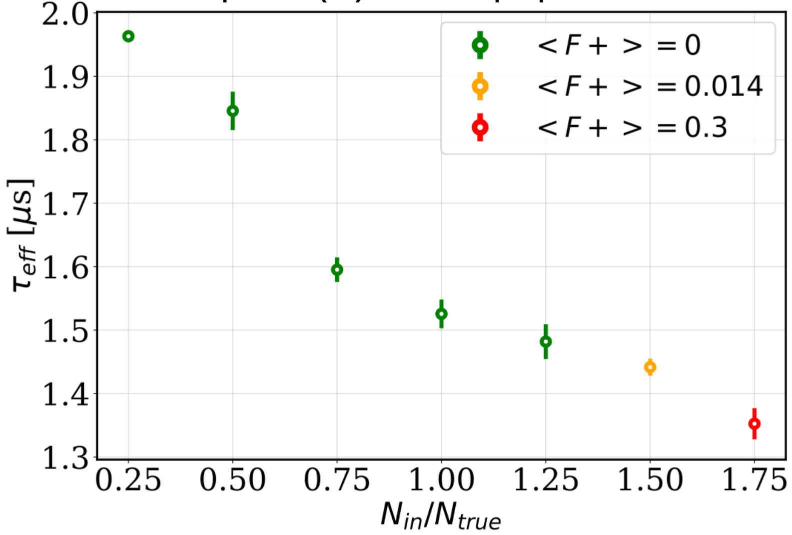

- Instead of using filters, the f_{pp} could be reduced by adding an external source of single events with energies inside the ROI ($L\alpha$ x rays of Pd, 2833 eV and 2839 eV)

- The number of Pd events recorded was varied, thus varying the initial fraction of pile-up events

ROI energy spectrum with Pd source

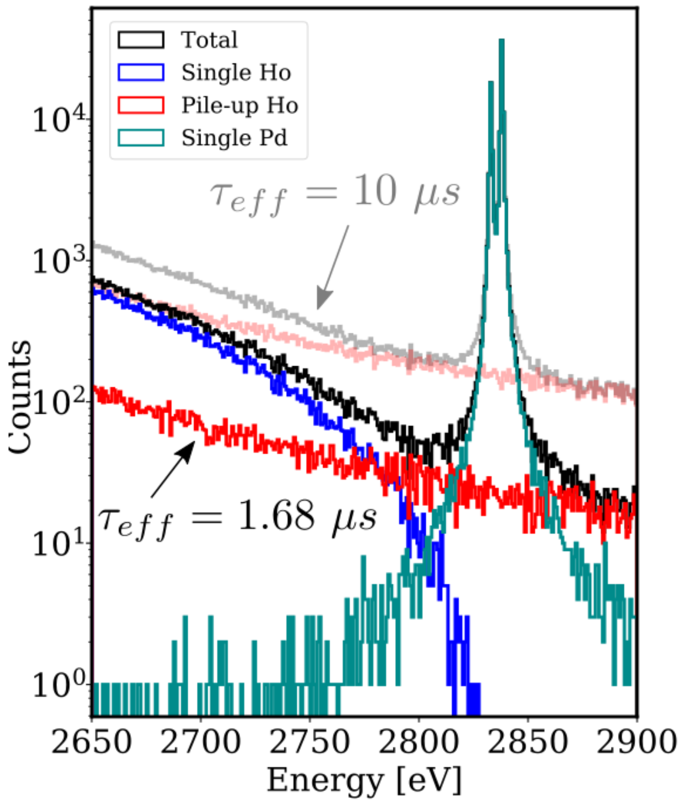

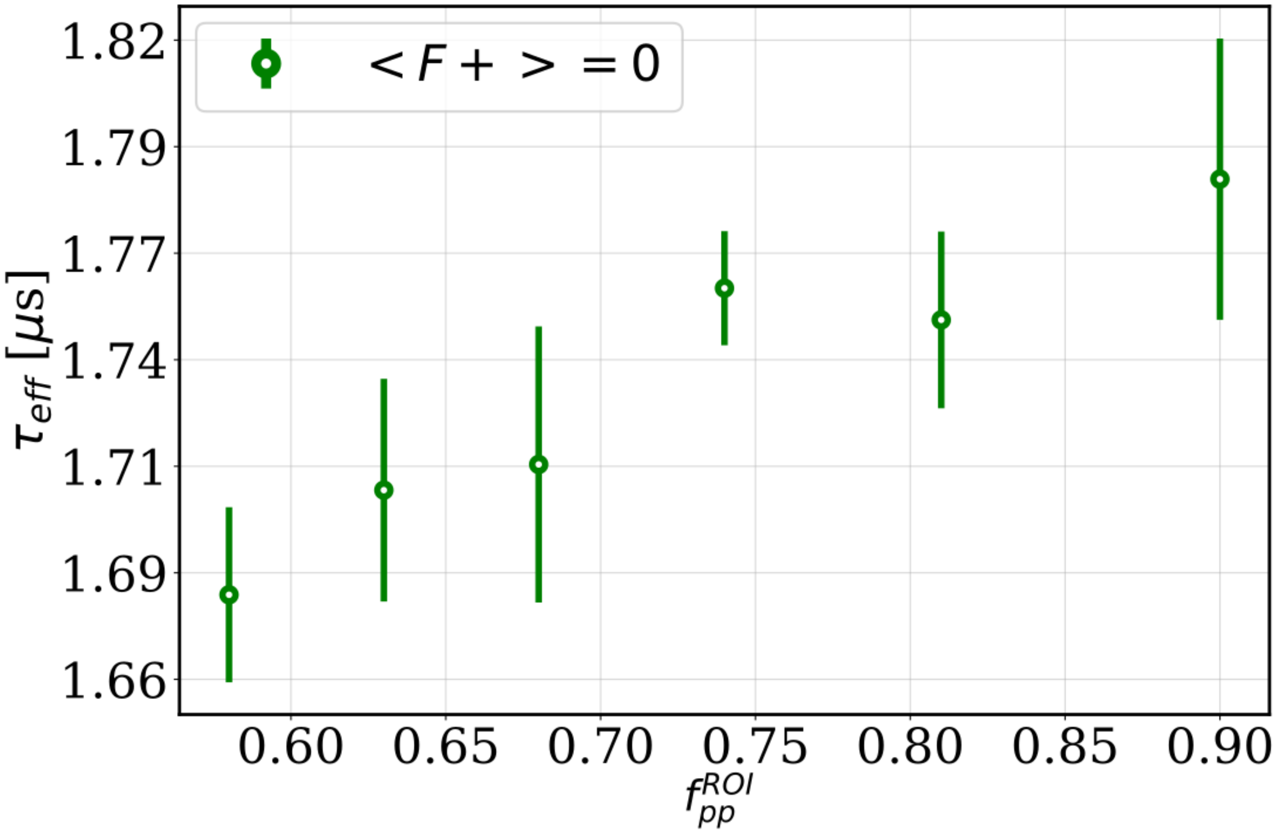

Lowering the pile-up fraction: DSVP final results

- With the target detector of HOLMES, the DSVP technique allows to reduce the f_{pp} from 10^{-3}($\sim \tau_{eff}$ $3\ \mu s$) to 10^{-4}($\sim \tau_{eff}$ $1.5\ \mu s$)
- Neutrino mass sensitivity improves from about 2 eV to about 1.4 eV.

Detector type	Rise time [μs]	t_{sample} $[\mu s]$	τ_{eff} $[\mu s]$ (WF)	τ_{eff} $[\mu s]$ (DSVP)
(b)	11	2	2.26	1.55
(b)	17	2	2.37	1.55
(b)	22	2	2.94	2.01
(b)	17	1	1.66	0.94
(a)	10	2	1.82	1.24
(c)	19	2	2.70	1.82